Hydraulic servo actuator control

SC42095 Control Engineering

Assignment 19-20

MSc Systems & Control
Delft University of Technology
Qingyi Ren 5684803
January 7, 2023

I. Introduction

The aim of this assignment is to find suitable control algorithms for hydraulic servo mechanisms shown in Fig 1. With proper design for controllers, large-mass hydraulic servo mechanisms shows a rapid response and satisfies different requirements in continuous-time domain as well as discrete-time domain.

Fig. 1. Hydraulic servo mechanisms.

II. Continuous-time control

In this section, the transfer function of hydraulic servo system with the position as output is given as:

$$G(s) = \frac{s^2 + 5s + 50}{(0.1s + 1)(s^2 + 2.5s + 25)}$$

From the third order transfer function, the zeros and poles are obtained and listed in table I

zeros	position
1	-2.50 + 6.61i
2	-2.50 - 6.61i
poles	position
1	-10
2	-1.25 + 4.84i
3	-1.25 - 4.84i

TABLE I
THE LOCATION OF ZEROS AND POLES OF TRANSFER FUNCTION.

through pole-zero map in Fig 2 one can clearly observe all the zeros and poles of the $3th$ open-loop transfer function $G(s)$ locate in the closed left-half plane thus we can conclude the hydraulic servo system is the minimum phase system which infers the stability of the system.

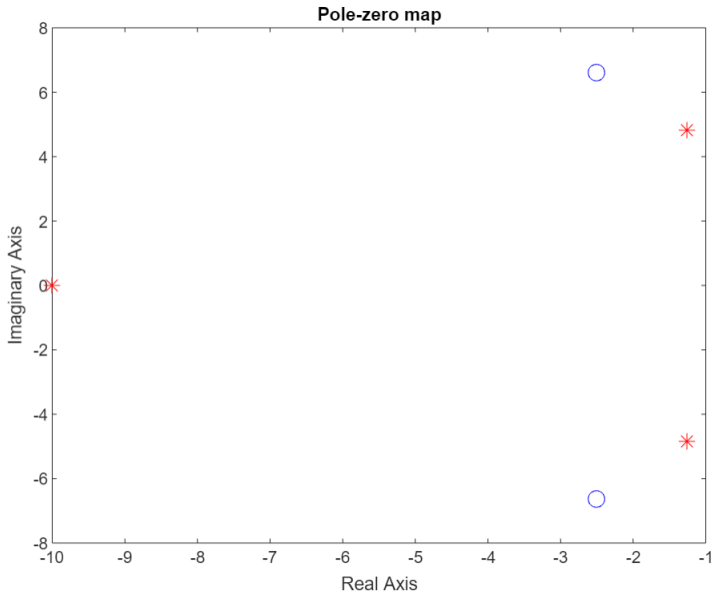

Fig. 2. Pole-zero map.

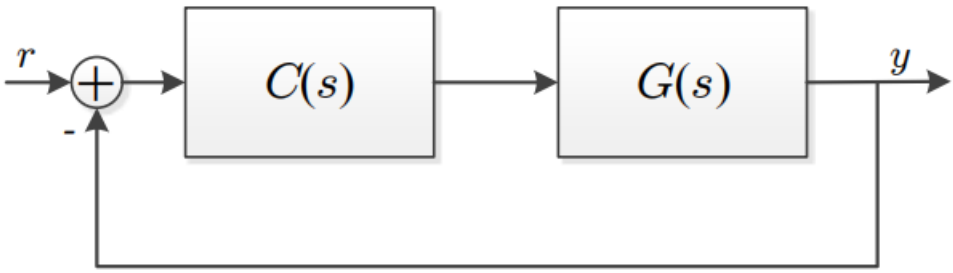

Fig. 3. Reference tracking system.

A. *Reference tracking controller*

In figure (3) where The $c(s)$ is the designed transfer function of PID controller, $G(s)$ is the transfer function of the plant. r, and y are the reference input and output signals added to the system respectively.

It is required that three control objectives of reference tracking controller need to be satisfied,

(a) minimal settling-time
(b) overshoot $< 5\%$
(c) steady-state error $= 0$

The steady state error of close-loop system can be computed as:

$$e(\infty) = \lim_{t\to\infty} e(t) = \lim_{s\to 0} sE(s) = \lim_{s\to 0} s\frac{R(s)}{1+G(s)} = \lim_{s\to 0}\frac{1}{1+G(s)} = \frac{1}{3}$$

Here we use step input $R(s) = \frac{1}{s}$. It can be seen that the system is type 0 and has non-zero steady error, thus integral action for the reference tracking is necessary, which means that controller structure need to be chosen from PI and PID. Fig 4 shows the Bode graph of the system. it can be seen that the phase curve start at 0° and the magnitude curve has a slightly increasing gain when the frequency $f \leq 4.49 rad/s$. According the bode plot, the plant was already stable with the G_m and P_m both greater than zero.

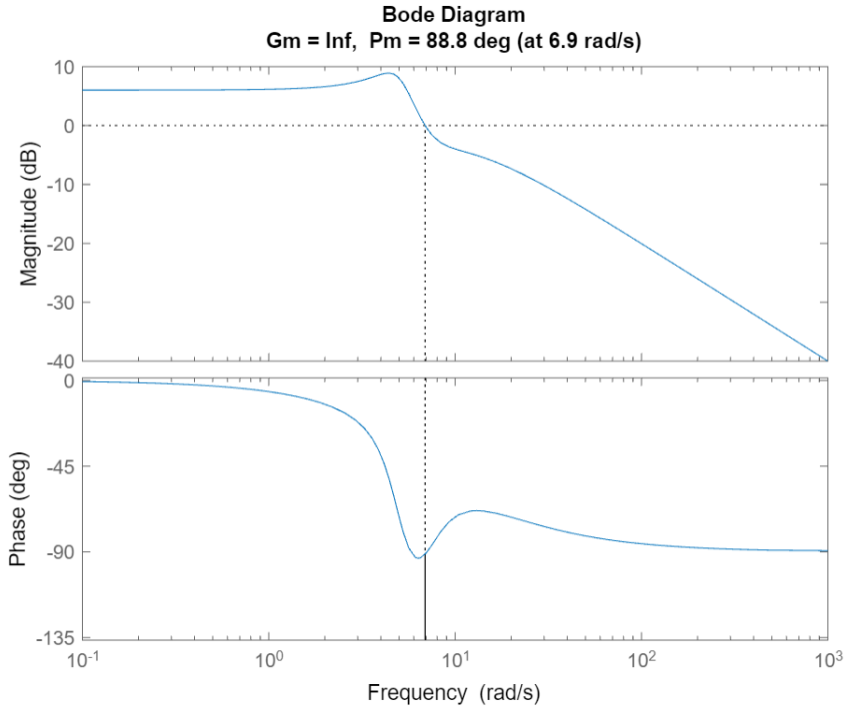

Fig. 4. Bode graph of the system.

In order to meet the needs of control objectives, the system was usually seen as the approximation of the second order system, from which the desired overshoot can be convert into the pole location.

Here we suppose the overshoot is 0.05, and apply the corresponding equation as followed:

$$\xi = \sqrt{\frac{(\ln 0.05)^2}{\pi^2 + (\ln 0.05)^2}} = 0.69 \tag{1}$$

And then compute the ω_n:

$$\omega_n = \frac{4}{T_s \xi} = \begin{cases} 5.8, T_s = 1 \\ 3.6, T_s = 1.6 \end{cases} \tag{2}$$

where T_s represents the settling time of the system. With the intermediate variables above we acquired, we can easily come to the desired poles:

$$-\omega_n \xi \pm i\omega_n \sqrt{1 - \xi^2} = \begin{cases} -4.0 \pm +4.2i, T_s = 1 \\ -2.5 \pm +2.6i, T_s = 1.6 \end{cases} \tag{3}$$

By observing the plant transfer function, there exists two pairs of complex zeros and poles which are close to each other. The pair of pole can be cancelled out by the pair of zero. The dominant pole of the plant can be viewed as $\frac{1}{0.1s+1}$, as the pairs of zero and pole has small effect of the system, the plant can be approximated as

$$G(s) \approx \frac{k}{s + 10} \tag{4}$$

where the k represents the DC gain after cancelling out the pairs of zero and pole.

As former analysis, to satisfy the control requirements, we already obtain the second order control system. In order to approximate the system's poles to the pair of desired complex pole. The controller could be written as the integral part multiplied by the lag compensator.

$$C(s) = \frac{K_I}{s} C_{compensator} \tag{5}$$

where $C_{compensator} = \frac{p}{z} \cdot \frac{s+z}{s+p}$, with $z > p$, z is the zero location and p is the pole location. Mention that in the original plant $G(s)$, the pair of poles are on the left of the pair of zeros, to compensate the negative phase caused by the location of poles on the left of zeros. The compensator needs to be lag compensator, because the zero of compensator is fixed at $s = -10$ to cancel out the pole existing in the plant transfer function. The pole of compensator can be designed by using the desired real part of complex second order poles $-p_{real} \pm ip_{img}$, which could be approximated as $(s + p_{real} + ip_{img})(s + p_{real} - ip_{img}) \approx s(s + 2p_{real})$.

1) Initial controller guess: By assuming the $T_s = 1.6$ sec, the real part of desired second order desired poles is -2.5. Then the pole of compensator can be designed as $s = -5$.

The PID controller is written as

$$C(s) = 0.475 \frac{s + 10}{s(s + 5)} \tag{6}$$

. The step response of the system is shown in figure (5). The performance of the discrete-time reference tracking controller is

(a) settling-time $= 3.16$ sec
(b) overshoot $= 4.95\%$
(c) steady-state error $= 0$

2) First iteration: In order to speed up the system, the settling time could be chosen as $T_s = 1$ sec. By assuming the $T_s = 1$ sec, the real part of desired second order desired poles is -4.

Then the pole of compensator can be designed as $s = -8$.

The PID controller is written as

$$C(s) = 0.79 \frac{s + 10}{s(s + 8)} \tag{7}$$

. The step response of the system is shown in figure (6). The performance of the discrete-time reference tracking controller is

(a) settling-time $= 3.61$ sec
(b) overshoot $= 4.98\%$
(c) steady-state error $= 0$

3) Final controller choice: In order to reduce the overshoot, inspired by the root locus method, $\sum \theta_z - \sum \theta_p = -180°$, where θ_z and θ_p represent the angle between the zero and the desired second order pole and the angle between the pole and the desired second order pole. As mentioned before, the pair of zeros of the plant is located on the left of the pair of poles of the plant. To compensate the angle change caused by the location of zeros and poles. The pole of the compensator could be moved to the left slightly.

Then by tuning the pole of compensator to the position -8.5, the PID controller is given as

$$C(s) = 0.8 \frac{s + 10}{s(s + 8.5)} \tag{8}$$

In figure (7), the performance of the discrete-time reference tracking controller is

(a) settling-time $= 3.05$ sec
(b) overshoot $= 4.19\%$

(c) steady-state error $= 0$

which satisfies the control objectives of reference tracking controller. Also by comparing with the initial guess and first iteration of PID controllers, the final choice of PID controller has the smallest overshoot and settling time, shown in figure (8).

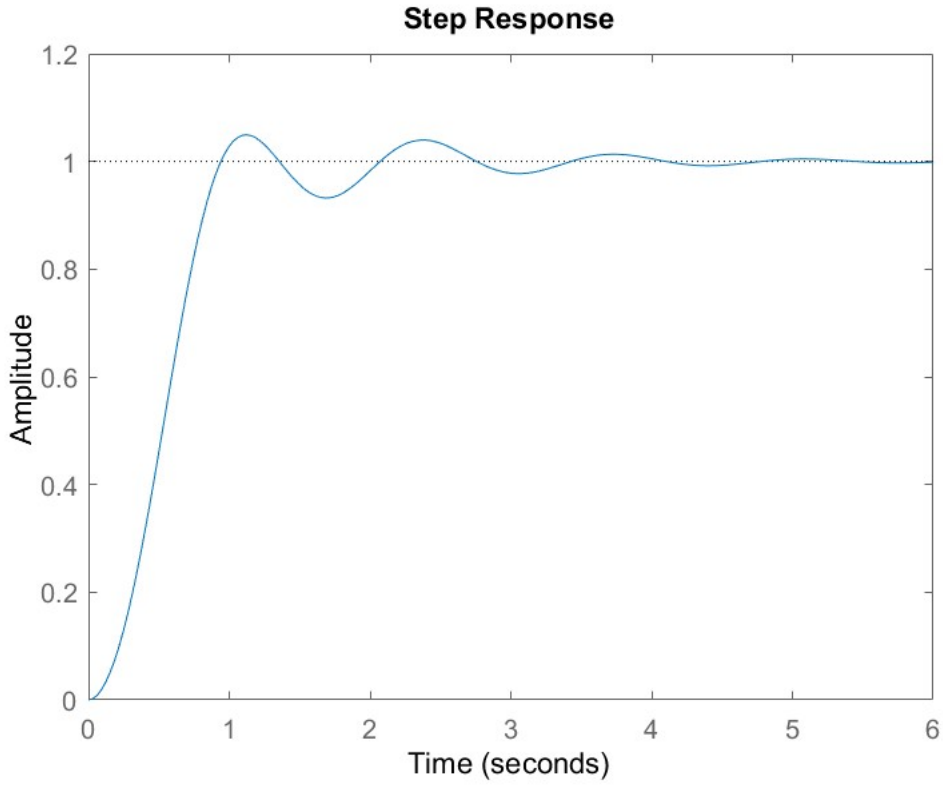

Fig. 5. Step response of initial guess for reference tracking.

B. Disturbance rejection controller

In this section, the disturbance rejection model is shown in figure (9). The $c(s)$ is the designed transfer function of PID controller, $G(s)$ is the transfer function of the plant. q, r, and y are the disturbance, reference input and output signals added to the system respectively. The transfer function of the disturbance rejection model is

$$\frac{Y(s)}{Q(s)} = \frac{G(s)}{1 + G(s)C(s)} \tag{9}$$

where $Y(s)$, $G(s)$, $C(s)$ and $Q(s)$ represent the Laplace transform of the output signal y, plant, PID controller for disturbance rejection respectively.

The control requirements of the PID controller of disturbance rejection are listed below:

(a) minimal amplitude of the system output y caused by disturbance q.
(b) minimal duration of the disturbance.
(c) no offset caused by the disturbance.

In order to achieve the requirement of no offset caused by the disturbance, in another word, the zero steady value of step response has to be achieved which implies the output y goes to zero when time goes

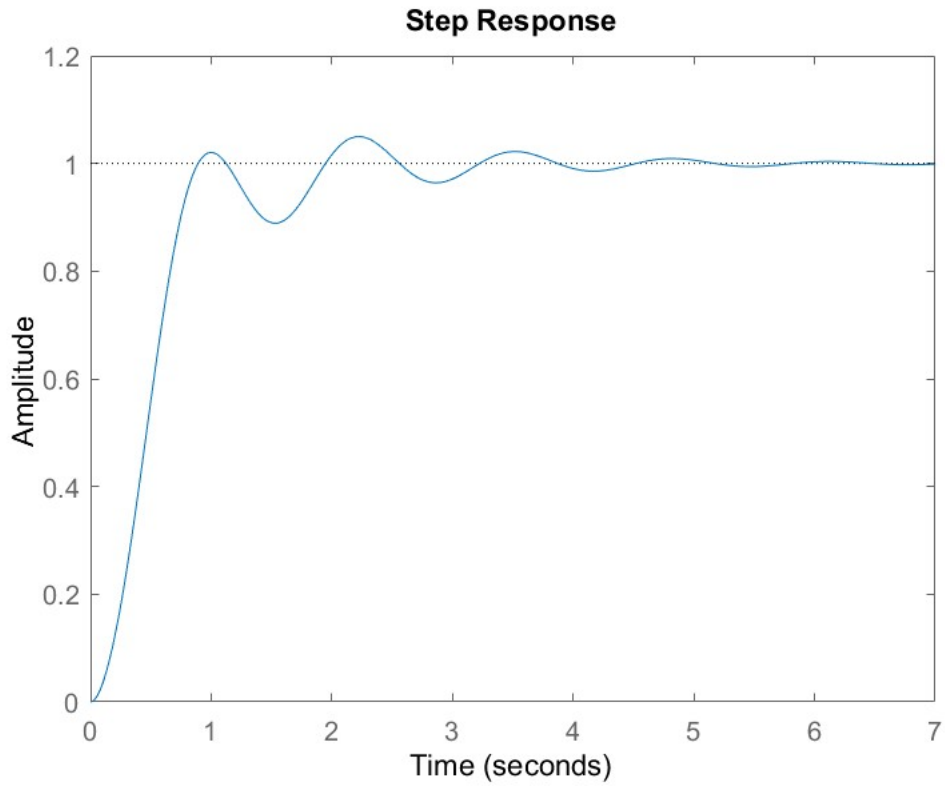

Fig. 6. Step response of first iteration for reference tracking.

to infinite. Then the input signal is step function which corresponds to Laplace transform $\frac{1}{s}$. The output y can be written as

$$\begin{aligned}\lim_{t\to\infty} y(t) = \lim_{s\to 0} sY(s) &= \lim_{s\to 0} s\frac{\frac{s^2+5s+50}{(0.1s+1)(s^2+2.5s+25)}}{1+\frac{s^2+5s+50}{(0.1s+1)(s^2+2.5s+25)}G(s)}\frac{1}{s} \\ &= \lim_{s\to 0}\frac{(s^2+2.5s+25)}{(0.1s+1)(s^2+2.5s+25)+(s^2+5s+50)G(s)} = \frac{25}{25+50G(s)}\end{aligned} \tag{10}$$

In order to achieve $\frac{25}{25+50G_d(s)} = 0$, the $G(s)$ has to contain a pure integrator, which will add one more zero to the numerator at the position 0. The $G(s)$ can be represented as $G(s) = H(s)/s$, then $\frac{25}{25+50G_d(s)}$ can be represented as $\frac{25s}{25s+50H(s)}$, when $s \to 0$, $\frac{25s}{25s+50H(s)} \to 0$. Similarly, the function $G(s)$ at least contains integrator part and the analysis started from I type controller.

The derivative element is needed because around 180 degree phase drops around the frequency $219rad/s$. The general approach of phase increase is to add the derivative element to PID controller.

The proportional controller is also needed because it can only change the magnitude of system with the phase of the system unchanged. In bode plot, the proportional controller can make the bode plot shift upwards or downwards by increasing or decreasing the proportional gain. This strategy can be used to change the crossover frequency and the phase margin of the system. In figure (10), the crossover frequency is $219rad/s$ and the focus can be put on changing the crossover frequency. Higher crossover frequency can yield a faster system response and thus makes the system have the small duration time. The other

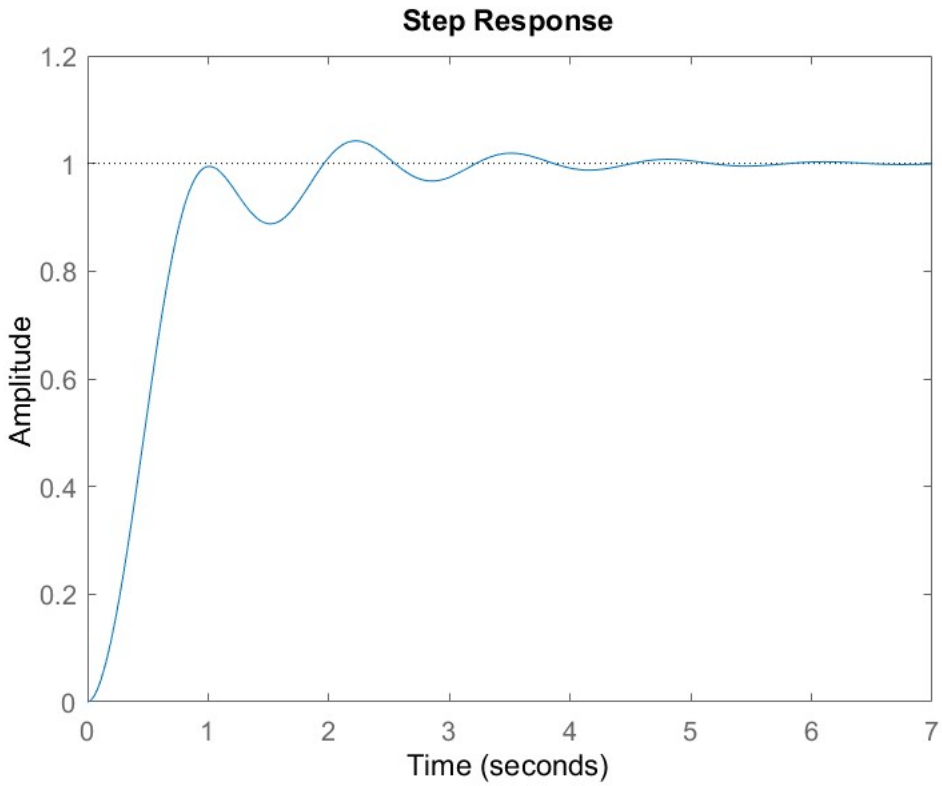

Fig. 7. Step response of final choice for reference tracking.

reason for the need of integrator is to reduce the amplitude of the step response. It is evident that in figure (11), the amplitude of the system output y caused by disturbance q is quite high. In order to solve this problem, K_P can be increased to reduce the phase margin in the proper range $[40°, 60°]$ which can avoid excessive oscillations.

The structure of PID controller is written as:

$$C_{PID} = K_P + \frac{K_I}{s} + \frac{K_D s}{T_f s + 1} \tag{11}$$

where K_P, K_I and K_D are proportional, integer and derivative gain respectively, T_f is the parameter to enhance the high frequencies performance of the derivative part.

1) Initial controller guess: In figure (11), it shows that the maximum magnitude of the step response of the disturbance rejection is and 0.0436 and it takes 0.625 sec to achieve reduce to within 1% of its maximal value. In this case, the K_I is set to 5000. The initial guess for PID controller $C(s)$ is shown in table II.

The step response of the system is shown in figure (12), it is easily observed that by adding the proportional and integral part to the system, the highest amplitude reduced to the value 0.0314, and the duration time reduced to 0.0402 sec.

2) First iteration: In order to keep on decreasing the highest amplitude of step response, the K_P should be increased. PID parameters for the first iteration controller is shown in table III. The step response of the system is shown in figure (13), it is found that the highest amplitude reduced to the value 0.00849, and the duration time reduced to 0.0307 sec.

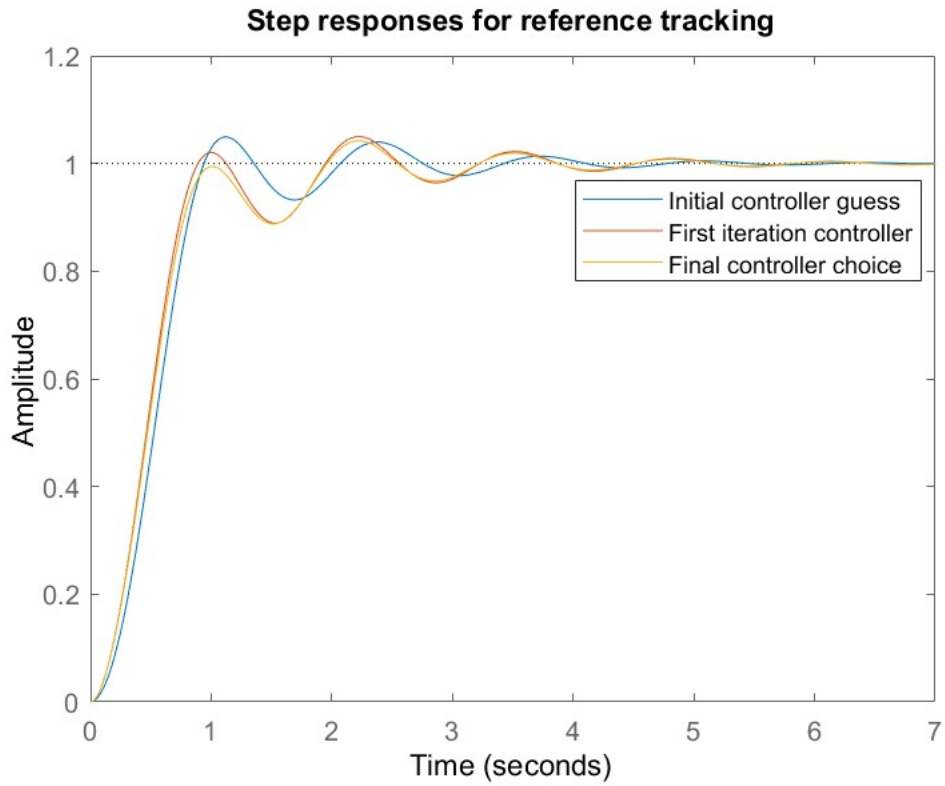

Fig. 8. Step responses of initial guess, first iteration and final choice for reference tracking.

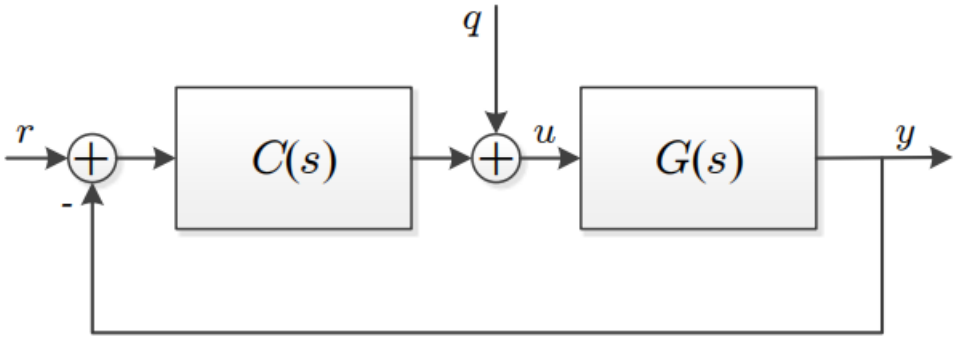

Fig. 9. Disturbance rejection model.

PID parameters	Values
K_P	10
K_I	5000
K_D	1
T_f	100

TABLE II
PID PARAMETERS FOR THE INITIAL CONTROLLER GUESS.

PID parameters	Values
K_P	100
K_I	5000
K_D	1
T_f	100

TABLE III
PID PARAMETERS FOR THE FIRST ITERATION CONTROLLER.

3) Final controller choice: For the goal of keeping on decreasing the amplitude of the step response without increasing the duration time. The integral and derivative parameters K_I and K_D are to be increased to decreased the highest amplitude and dynamics of step response.

The step response of the system is shown in figure (14), it is found that the highest amplitude reduced to the value 0.00821, and the duration time reduced to 0.0314 sec. Note that even the final choice system's duration time is larger than that of the first iteration, the curve of the step response of the final choice is inside that of the first iteration, which means at each time point, the output value y of final choice system is smaller than that of the first iteration system.

Overall, the comparison of step responses using different PID controllers is shown in figure (15). By tuning the PID parameters properly, the final choice of the PID controller shows better performance compared with the initial guess controller and first iteration controller and satisfies the control objectives.

PID parameters	Values
K_P	100
K_I	8000
K_D	5
T_f	100

TABLE IV
PID PARAMETERS FOR THE FINAL CHOICE CONTROLLER.

The final performance of the PID controller is shown as:

(a) duration time $= 0.0314$ sec
(b) Amplitude of the system output y caused by disturbance q: 0.00821
(c) steady output $y = 0$

which satisfies the control objectives of disturbance rejection controller.

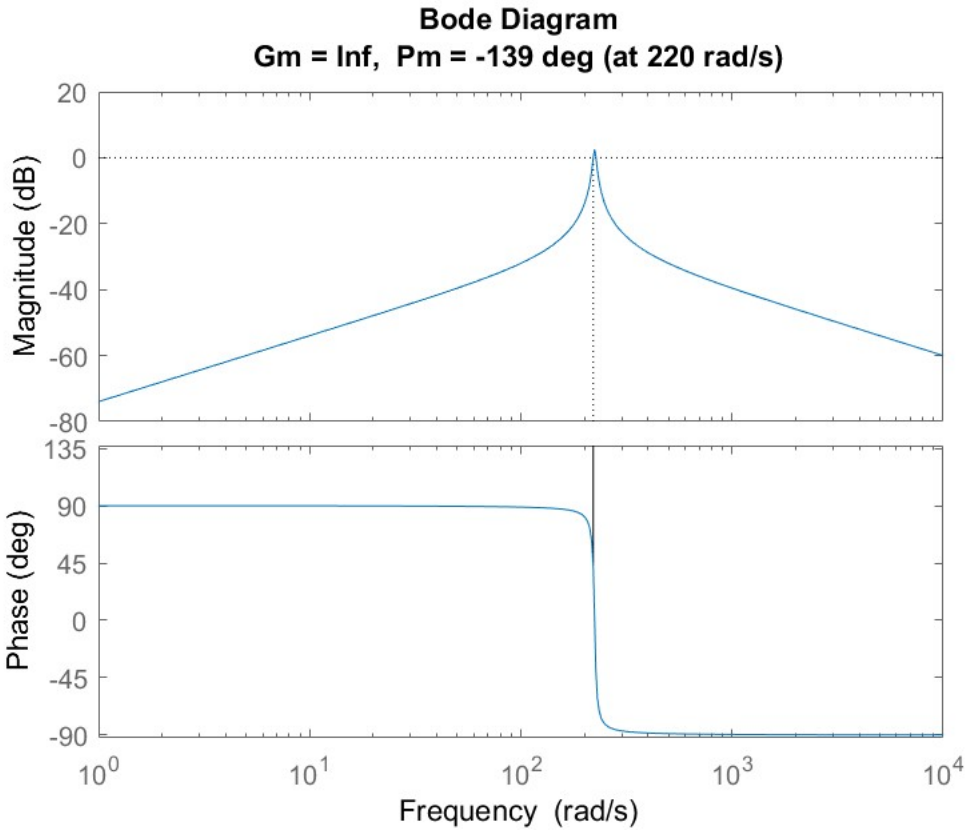

Fig. 10. Bode graph of the disturbance rejection system.

III. Discrete-time control

A. *Discrete-time state space model*

The continuous-time state space model is written as

$$\begin{aligned} \dot{x} &= Ax + Bu \\ y &= Cx + Du \end{aligned} \tag{12}$$

For obtaining the matrices of A, B, C and D, the MATLAB command **tf2ss** is firstly used to get the structure of the continuous-time state space model from the the transfer function of the system. The matrices of A, B, C and D are shown as,

$$\begin{aligned} A &= \begin{bmatrix} -12.5 & -50 & -250 \\ 1 & 0 & 0 \\ 0 & 1 & 0 \end{bmatrix} \\ B &= \begin{bmatrix} 1 \\ 0 \\ 0 \end{bmatrix}, C = \begin{bmatrix} 10 & 50 & 500 \end{bmatrix}, D = 0 \end{aligned} \tag{13}$$

Because the transfer function depicts servo system with the position as output. According to the knowledge of transfer function, the states x_2 and x_3 are the integral to the state x_1 and x_2. The output y represents the position of the motor and is the weighted combination of x_1, x_2 and x_3. Taking the structure of the

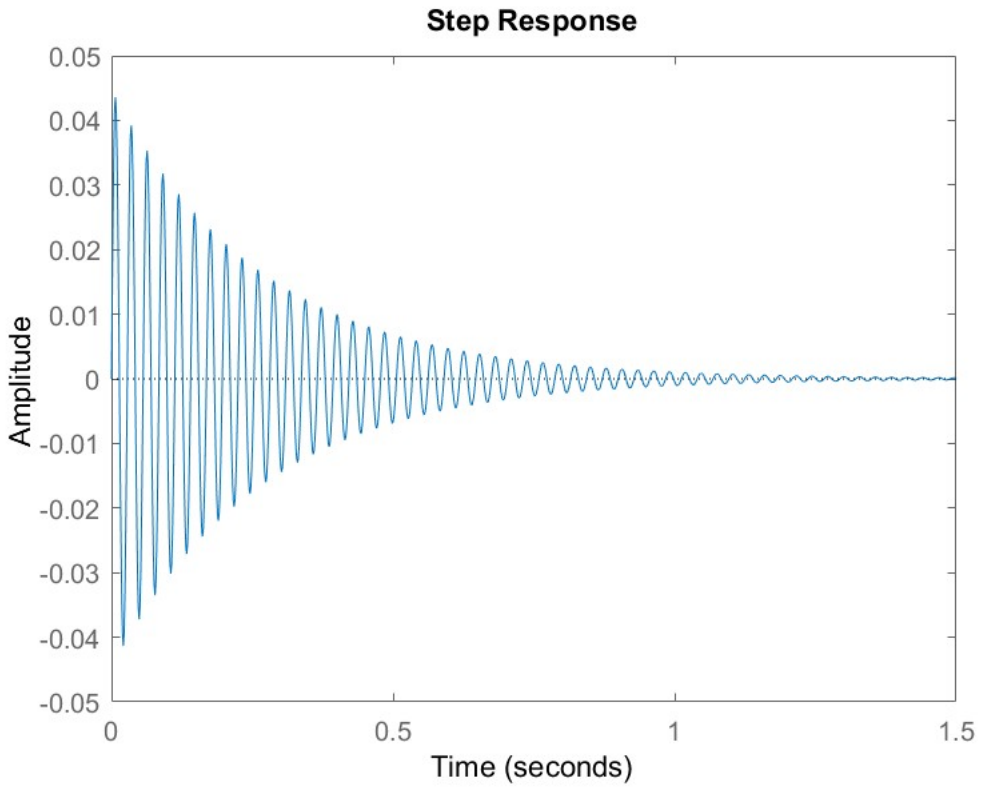

Fig. 11. Step response of the disturbance rejection system.

servo system into consideration and the architecture of servo system, the physical description of each states are depicted as

- x_1: motor current.
- x_2: angular velocity.
- x_3: angular position.

Secondly, in order to obtain the discrete-time state space model, a suitable sampling time needs to be selected to discretize the continuous-time state space model. Taking into account the balance between the high sampling time which can capture the dynamics of the system and low sampling time which can prevent the side effects introduced by oversampling, the proper sampling time is defined as

$$h \leq h_{max} = \frac{2\pi}{4 \cdot 2} = 0.785s \tag{14}$$

The formula (14) provides the general upper bound for choosing the sampling time. When the focus put on specific systems, and designing the fitting sampling time for the system, another formula which is usually employed as the rule of thumb for the sampling period has the form of

$$h \approx \frac{h_{rise}}{8} \tag{15}$$

where h_{rise} can be obtained by doing the experiment of the step response of the system, and h_{rise} represents the rise time of step response. The obtained value was reduced by checking the step response and the observation of a clear oversampling and therefore, the above-mentioned rule of thumb for the sampling

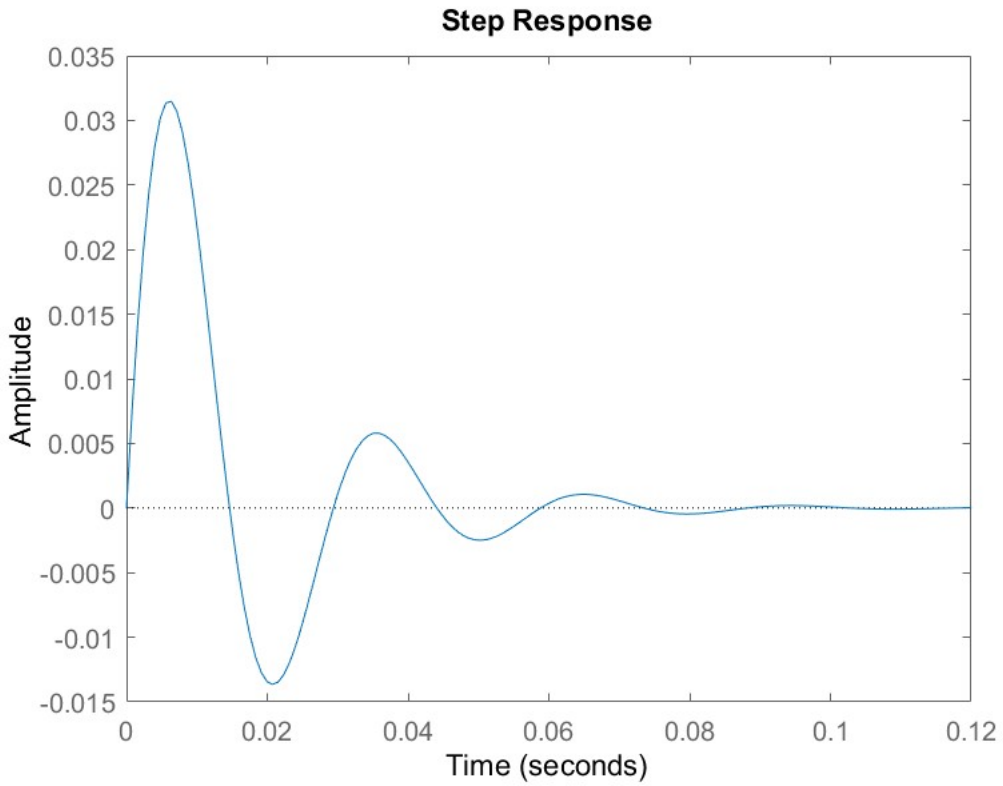

Fig. 12. Step response of initial guess of the disturbance rejection system.

period was applied. In this part, the sampling time is chosen as $h = 0.074375$ s, the discrete-time state space model is showed as

$$\begin{aligned} x(k+1) &= \Phi x(k) + \Gamma u(k) \\ y(k) &= Cx(k) + Du(k) \end{aligned} \tag{16}$$

By using the MATLAB command **c2d**, the matrices can be obtained as,

$$\Phi = \begin{bmatrix} 0.3095 & -2.809 & -11.51 \\ 0.04604 & 0.885 & -0.507 \\ 0.002028 & 0.07139 & 0.9864 \end{bmatrix}, \Gamma = \begin{bmatrix} 0.04604 \\ 0.002028 \\ 5.445 \times 10^{-5} \end{bmatrix}, C = \begin{bmatrix} 10 & 50 & 500 \end{bmatrix}, D = 0 \tag{17}$$

B. Discrete-time Reference tracking controller

According the rise time of continuous time 0.595 sec, the sampling time is properly chosen as $h = 0.595/16 = 0.0325$ sec.

$$\frac{0.01328z^2 + 0.003712z - 0.009566}{z^2 - 1.757z + 0.7573} \tag{18}$$

.

In figure (16), it illustrates comparison of the continuous-time and discrete-time reference tracking system's step response. The discrete-time response can capture the dynamics of the system, with the shape of discrete-time response almost overlapping with the continuous-time response.

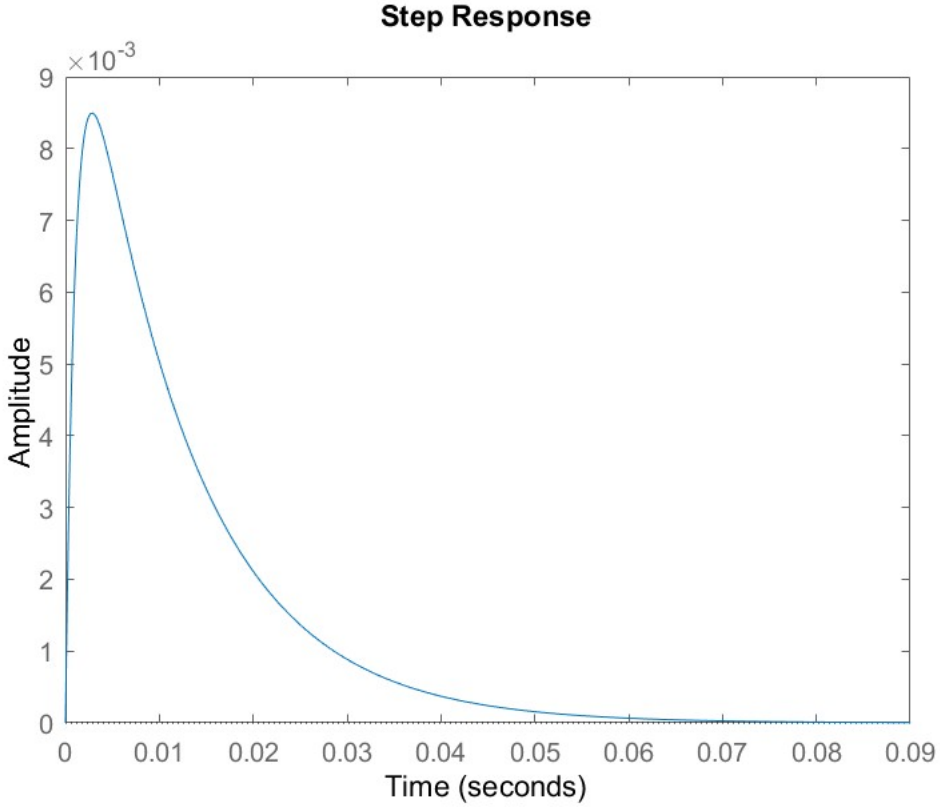

Fig. 13. Step response of first iteration for disturbance rejection.

C. Discrete-time Disturbance rejection controller

For disturbance rejection system model, it is not practical to choose suitable sampling time according to the formula (15) (not having rise time of continuous-time disturbance rejection model). Thus the trial and error are to be used to choose the optimal sampling time. The sampling time is chosen from the set $[0.0001, 0.0002, 0.0005, 0.0008, 0.001]$, and the step responses are shown in figure (17), compared with the continuous-time step response. It is observed that when the sampling time is relatively small, the discrete-time step response will match continuous-time response, in another word, the dynamics of system can be wholly captured. However the oversampling issue needs to be taken into account, which means the sampling time cannot be chosen too small. When the sampling time becomes larger, there will exist derivation from the continuous-time response, specifically having the larger corresponding peak value of step response. Overall, in order to balance the need to better capture the dynamics of system: fitting the continuous-time step response to the large extent and also try to avoid oversampling of the system.

Note that, when increasing the sampling time to the value of 0.005, the system is not stable and not converging any more, and the amplitude of step response goes to the very large value of $5 \cdot 10^5 8$, shown in figure (18).

Sampling time $h = 0.0005$

$$\frac{106.9z^2 - 204.8z + 98.1}{z^2 - 1.951z + 0.9512} \tag{19}$$

.

In figure (19), it illustrates comparison of the continuous-time and discrete-time reference tracking system's step response.

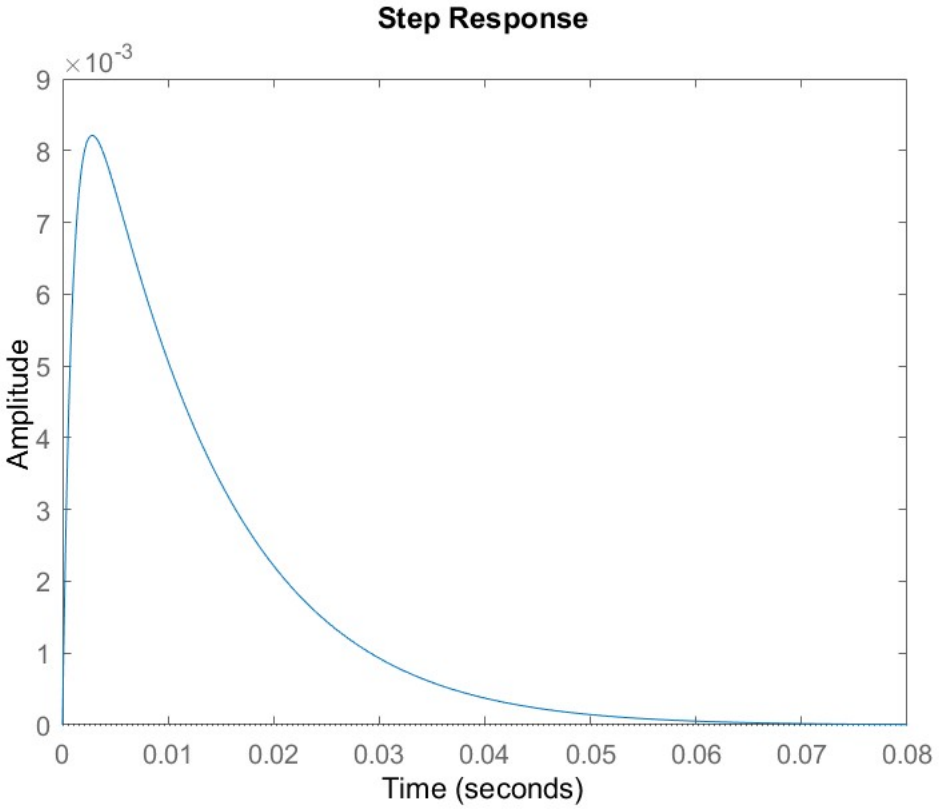

Fig. 14. Step response of final choice for disturbance rejection.

IV. Discrete-time State-Feedback control

In this part, the system is controlled by the state-feedback controller by the pole placement method. The main concept is to introduce the input in the form of $u = -Kx$. The prerequisite of constructing the state-feedback controller is the controllability of the pair (Φ, Γ), by using the MATLAB function **ctrbf**. Firstly, the second order poles are designed as dominant poles of the third order system (having three poles) based on the control requirements and the remaining one pole is placed as far as possible away from the designed second order poles, which decreases the side influence of nondominant poles on the performance of control requirements.

The continuous-time second order poles can be obtained by:

$$\begin{aligned} p_1 &= \zeta w_n + j w_n \sqrt{1-\zeta^2} \\ p_1 &= \zeta w_n - j w_n \sqrt{1-\zeta^2} \end{aligned} \tag{20}$$

where ζ is damping ratio and w_n is the natural frequency. The damping ratio is defined by the overshoot (21). The natural frequency w_n has the dependence of ζ and settling time t_s as shown in equation (22). The settling time is connected with the bandwidth w_B in equation (23)

$$os = 100 e^{\frac{-\zeta\pi}{\sqrt{1-\zeta^2}}} \tag{21}$$

$$t_s = \frac{-ln(0.02)}{\zeta w_n} \tag{22}$$

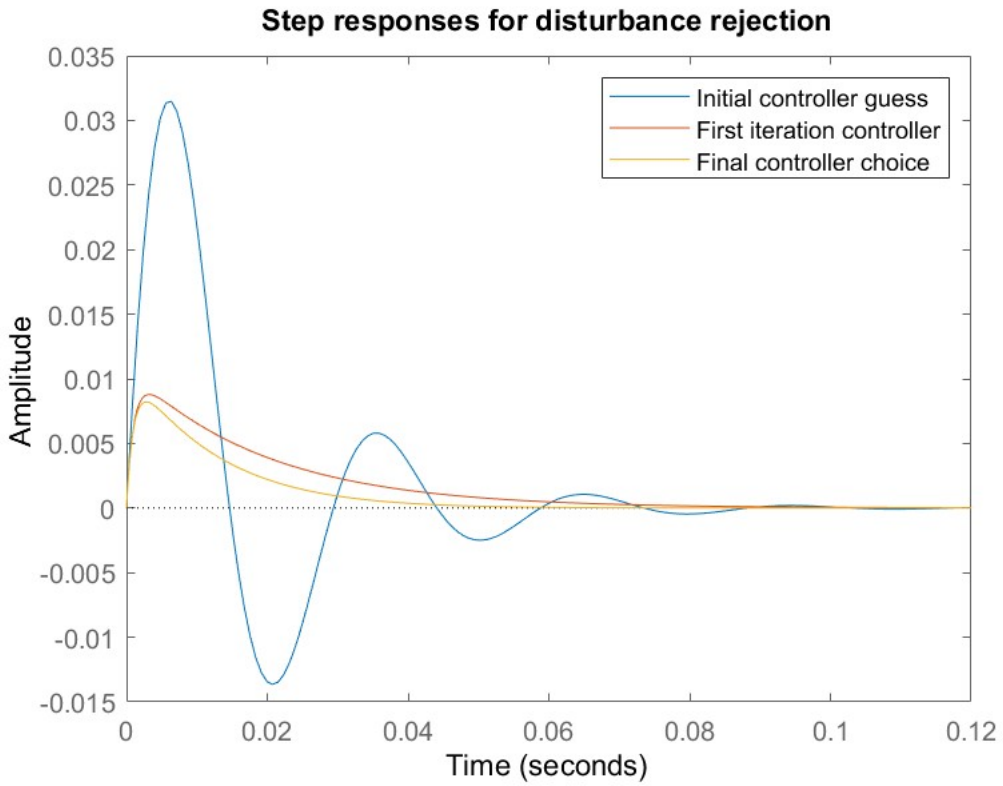

Fig. 15. Comparison of step response for disturbance rejection by using different PID controllers.

Poles set number	pole 1	pole 2	pole 3
1	$-0.6431 - 0.6744i$	$-0.6431 + 0.6744i$	-10.0000
2	$-1.2862 - 1.3488i$	$-1.2862 + 1.3488i$	-10.0000
3	$-3.2155 - 3.3721i$	$-3.2155 + 3.3721i$	-10.0000
4	$-6.4309 - 6.7442i$	$-6.4309 + 6.7442i$	-20.0000

TABLE V

FOUR DIFFERENT SETS s_1, s_2, s_3 AND s_4 OF CONTINUOUS-TIME POLE LOCATION.

$$t_s = \frac{4}{w_B \zeta^2} \sqrt{(1 - 2\zeta^2) + \sqrt{\zeta^4 - 4\zeta^2 + 2}} \tag{23}$$

Note that the bandwidth is not provided, thus the set of bandwidth is formulated $w_B = [1, 2, 5, 10]$ which constructs the four different sets of pole location. Starting from the maximum overshoot value 5%, the five different sets s_1, s_2, s_3, s_4 and s_5 of continuous-time pole location are calculated according to the equations (21), (22) and (23), shown in Table V.

In order to obtain the discrete pole location, the ZOH approximation is employed as

$$z = e^{sh} \tag{24}$$

, where h can be obtained according to the equation (15) and s represents the continuous-time pole location, z is the transformed discrete-time pole location. The five different sets s_1, s_2, s_3 and s_4 of discrete-time pole location are listed in Table VI. By using the MATLAB command **Place**, four controlled systems are obtained by using the four different poles sets. The step responses of four different controlled systems are

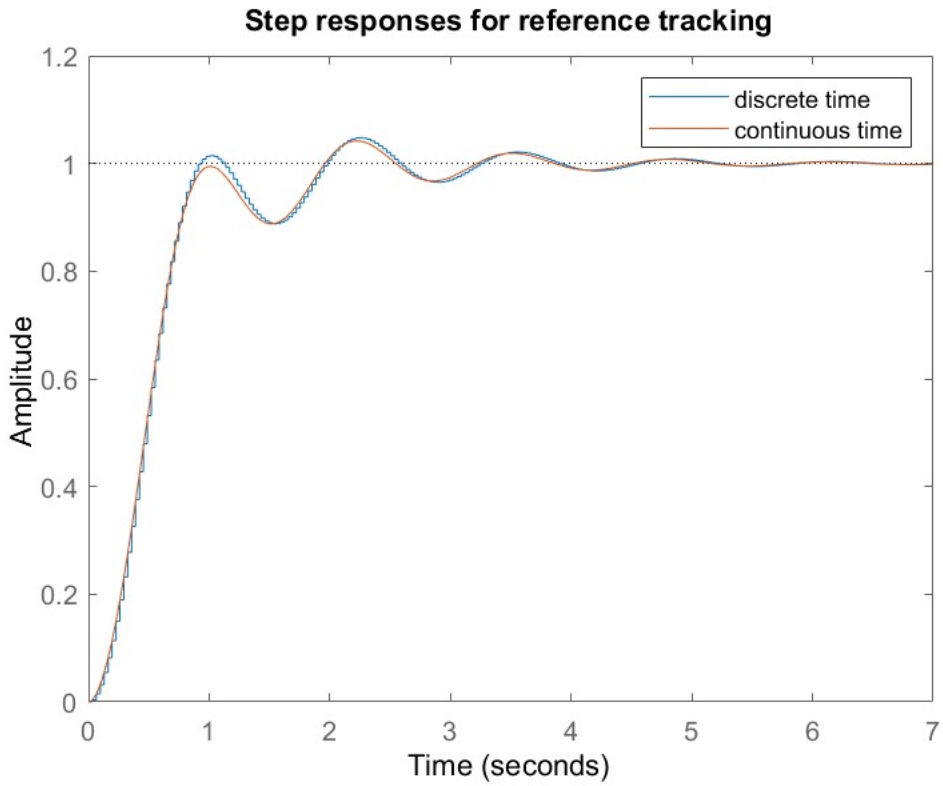

Fig. 16. Step response for reference tracking.

Poles set number	pole 1	pole 2	pole 3
1	$0.9759 - 0.0246i$	$0.9759 + 0.0246i$	0.6877
2	$0.9518 - 0.0481i$	$0.9518 + 0.0481i$	0.6877
3	$0.8795 - 0.1116i$	$0.8795 + 0.1116i$	0.6877
4	$0.7611 - 0.1964i$	$0.7611 + 0.1964i$	0.473

TABLE VI
FOUR DIFFERENT SETS s_1, s_2, s_3 AND s_4 OF DISCRETE-TIME POLE LOCATION.

shown in Fig 20, it is observed the step response of the third poles set is the relatively fast and can satisfy the control requirements, with the overshoot below 5%. Therefore, the bandwidth $w_B = 5$ is chosen, the discrete-time poles are $[0.8795 - 0.1116i, 0.8795 + 0.1116i, 0.6877]$.

Based on it, the optimal choice for designing the state feedback gain is obtained as $K = \begin{bmatrix} 5.5616 & 54.2847 & 49.9321 \end{bmatrix}$. The performance of the discrete-time state-feedback controller is

(a) settling-time $= 1.17$ sec
(b) overshoot $= 2.01\%$
(c) steady-state error $= 0$

which satisfies the control objectives of reference tracking controller.

V. OUTPUT-FEEDBACK CONTROL

The output feedback controller receives information from the original system and

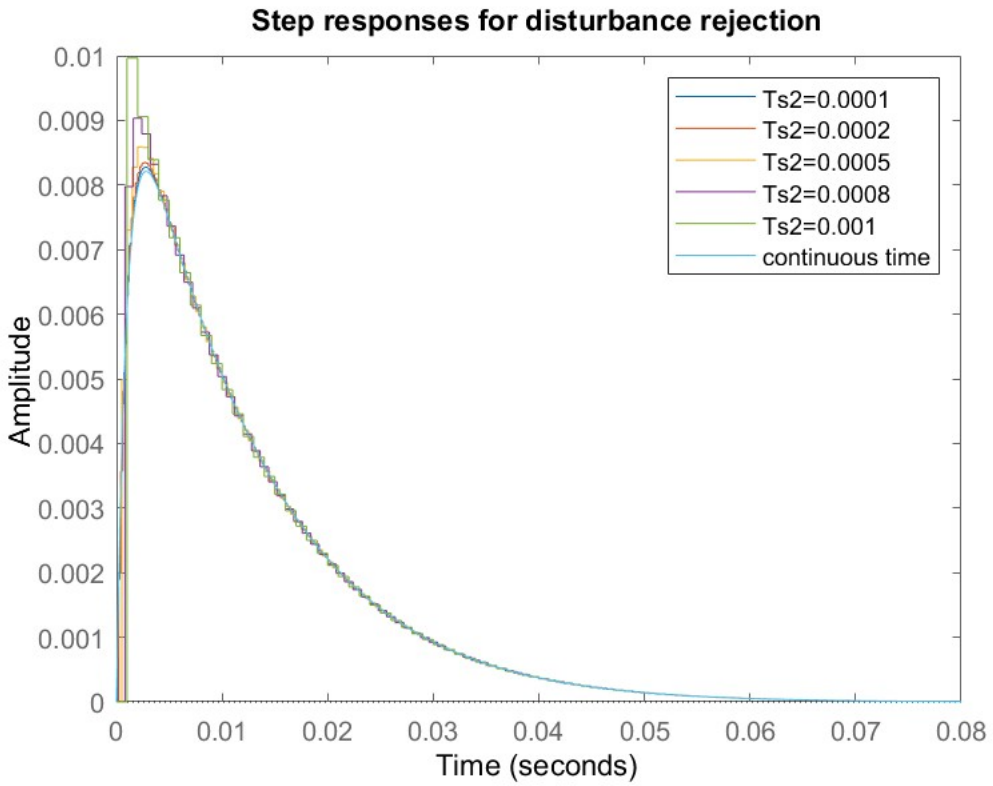

Fig. 17. Discrete-time step response for disturbance rejection by using different sampling time compared with the continuous-time step response.

A. *Output-Feedback Servo tracking controller*

The output-feedback servo tracking controller is designed in this part to stabilize the system and track the inputs. The output-feedback controller is constructed in the form

$$\hat{x}(k+1) = \Phi\hat{x}(k) + \Gamma u(k) + L(y(k) - \hat{y}(k)) \tag{25}$$

$$\hat{y}(k) = C\hat{x}(k) \tag{26}$$

where L is the Luenberger observer gain. The dynamics of estimate of the system is constructed as:

$$\hat{x}(k+1) = \Phi\hat{x}(k) + \Gamma u(k) \tag{27}$$

The estimation error is written as $\tilde{x}(k) = x(k) - \hat{x}(k)$. Combined withe the equation (27), the dynamics of the estimation error is defined as

$$\begin{aligned}\tilde{x}(k+1) = x(k+1) - \hat{x}(k+1) &= \Phi x(k) + \Gamma u(k) - \Phi\hat{x}(k) - \Gamma u(k) - L(y(k) - \hat{y}(k)) \\ &= \Phi(x(k) - \hat{x}(k)) - LC(x(k) - \hat{x}(k)) \\ &= (\Phi - LC)\tilde{x}(k)\end{aligned} \tag{28}$$

It is emphasized that to meet the need of asymptotically reconstruct the state, the full-information feedback is used and has the structure

$$u(k) = -K\hat{x}(k) + Gr \tag{29}$$

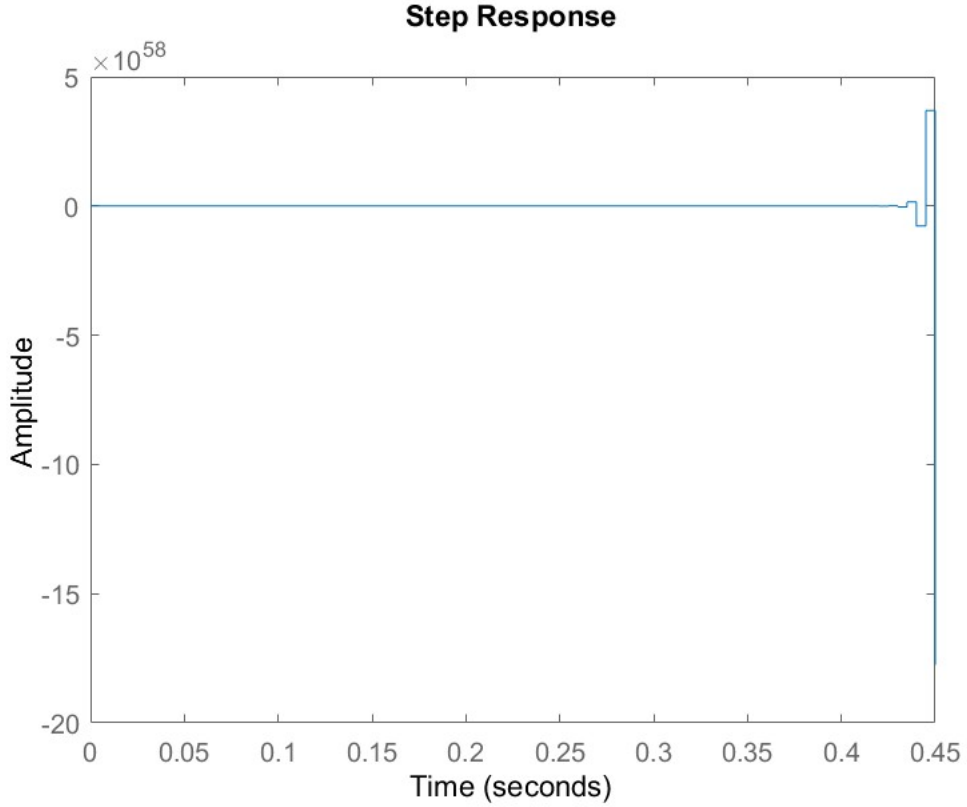

Fig. 18. Discrete-time step response for disturbance rejection by using different sampling time.

where r is the reference of the system, K is the state-feedback gain and G is the feedforward gain. Firstly, the Kalman matrix $\begin{pmatrix}\Gamma & \Gamma\Phi & \dots & \Gamma\Phi^{n-1}\end{pmatrix}$ is needed to be checked if it is full row rank which determines the controllability of the system. By using the MATLAB function **ctrbf**, that the controllability of the system guarantees that the poles of the dynamics of the estimate of the system (27) can be freely placed by designing the state-feedback gain K properly, in the form of $u(k) = -K\hat{x}(k)$. The location of the poles of $\Phi - \Gamma K$ determines how fast the system with state-feedback can react to the dynamics of the input, as defined in (30). At the same time, the pair (Φ, C) needs to be observable which makes sure the poles of the dynamics of the estimation error (28) can be placed freely by constructing the observer gain L properly, with the help of the MATLAB function **obsv**. The location of poles of $\Phi - LC$ determines the convergence rate of estimation error, if it is further into the left half plane, the dynamics of estimation error will become faster.

$$\dot{x}(k) = (\Phi - \Gamma K)u + \Gamma G r \tag{30}$$

Adding the observer dynamics to the state space model, the new close-loop state space model is written as

$$\begin{bmatrix} x(k+1) \\ \hat{x}(k+1) \end{bmatrix} = \begin{bmatrix} \Phi & -\Gamma K \\ LC & \Phi - \Gamma K - LC \end{bmatrix} \begin{bmatrix} x(k) \\ \hat{x}(k) \end{bmatrix} + \begin{bmatrix} \Gamma G \\ \Gamma G \end{bmatrix} r \tag{31}$$

From the former analysis, the state-feedback gain is already designed as $K = \begin{bmatrix} 5.5616 & 54.2847 & 49.9321 \end{bmatrix}$. Because of the full-information feedback structure, the feed-forward gain G needs to be designed to amplify the reference signal in order to decrease the steady state error caused by the state-feedback

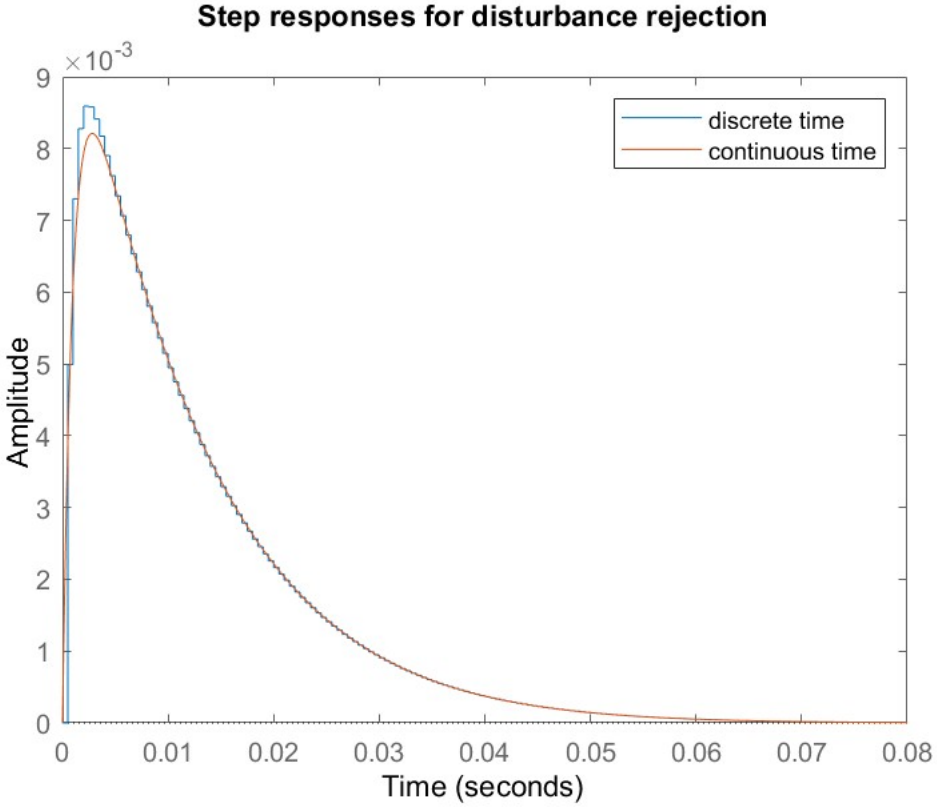

Fig. 19. Step response for disturbance rejection.

control. The given formula is equation (32)

$$G = \frac{1}{C(I - (\Phi - \Gamma K))^{-1}\Gamma + D} \tag{32}$$

Similar to the way of obtaining the state-feedback gain, the output-feedback gain is designed by choosing the poles for the observer separately. Taking the consideration of the dynamics of estimation error should be designed faster than that of the response to the input, the location of poles of $\Phi - LC$ should be designed on the left to the location of poles of observer, by the method of tuning L. Thus the poles of observer is listed:

- Continuous time domain $poles_{observer} = \begin{bmatrix} -11 & -12 & -13 \end{bmatrix}$

According to the equation (24), the continuous time pole location of the observer $poles_{observer}$ can be transformed to the discrete-time pole location $poles_{observer}$

- Discrete-time domain $poles_{observer} = \begin{bmatrix} 0.6624 & 0.6381 & 0.6147 \end{bmatrix}$

By choosing the initial state $x_0 = \begin{bmatrix} 0.001 & 0.001 & 0.001 \end{bmatrix}$, the step responses of system output and observer output are shown in figure (21) respectively. It shows that observer output can track the system's output properly. The initial states of the system output and observer output are the same because they both comes from the same initial states x_0. After 0.49 sec, the two systems' output are almost the same. It can be concluded that the design of state estimate based on the observers is high-speed and well fitted. The final value of the two systems' output have zero steady state, the peak exists in the curve accounts for the estimation error of states which slows down the process of the system converging to the final reference value and has bigger settling time.

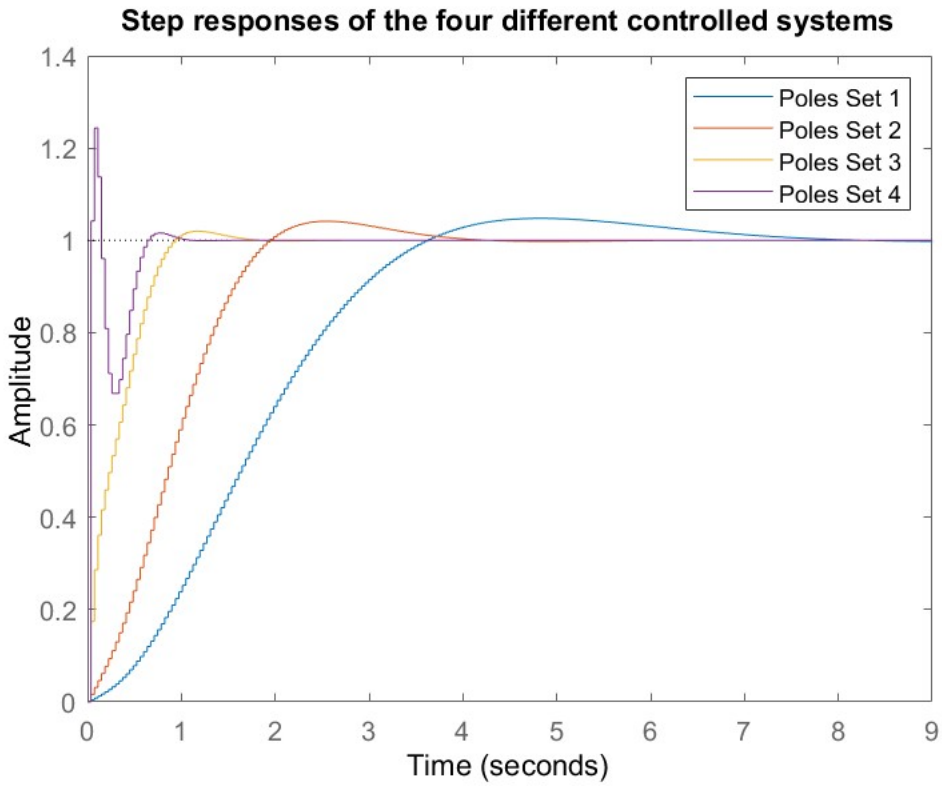

Fig. 20. Step responses of the four different controlled systems using different poles sets.

In figure (22), it compares the derivation of estimated states from the real states. It is observed that the error of state x_3 shows the higher resistance to the same amount of initial derivation from zero compared with states x_1 and x_2. After 0.52 sec, the error of states x_1, x_2 and x_3 converges to zero, which shows the good performance of the design of observer. Thus it can be concluded that the observer design is an ideal estimate of all the states. In another word, the observer can reduce the error of states by tracking the dynamics of the real states. The performance of the Output-Feedback servo tracking controller is shown as:

(a) settling-time $= 1.19$ sec
(b) overshoot $= 2.3\%$
(c) steady-state error $= 0$

which satisfies the control objectives of the reference tracking controller.

B. Output-Feedback disturbance rejection controller

In this part, the Output-Feedback disturbance rejection controller has an extended form including the disturbance plant input element w compared with the Output-Feedback Servo tracking controller.

The state equation is defined as:

$$x(k+1) = \Phi x(k) + \Gamma(u(k) + w(k)) = \Phi x(k) + \Gamma u(k) + \Gamma w(k) \tag{33}$$

Adding the disturbance dynamics $w(k+1) = w(k)$ to the state-space model, the augmented state-space model is shown as,

$$\begin{bmatrix} x(k+1) \\ w(k+1) \end{bmatrix} = \begin{bmatrix} \Phi & \Gamma \\ 0 & 1 \end{bmatrix} \begin{bmatrix} x(k) \\ w(k) \end{bmatrix} + \begin{bmatrix} \Gamma u(k) \\ 0 \end{bmatrix} \tag{34}$$

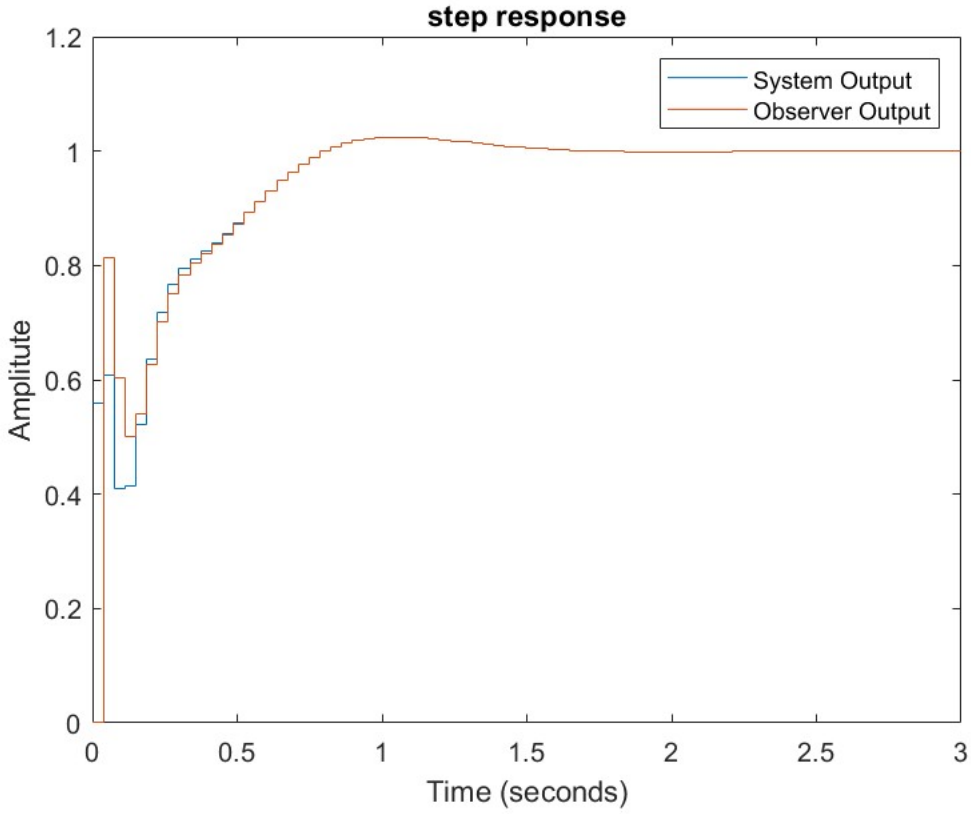

Fig. 21. Step responses of original system and observer system.

It easily observed that, the evolution of $w(k)$ cannot be influenced by input $u(k)$, which means $w(k)$ is uncontrollable. Then the control input also has extra disturbance element compared with the full-information feedback input, in the form of

$$u(k) = -K\hat{x}(k) - \hat{w}(k) + Gr \tag{35}$$

where $\hat{x}(k)$ and $\hat{w}(k)$ are the Luenberger observers of the state and disturbance respectively,

$$\begin{aligned} \hat{x}(k+1) &= \Phi\hat{x}(k) + \Gamma(\hat{w}(k) + u(k)) + L_x(y(k) - C\hat{x}(k)) \\ \hat{w}(k+1) &= \hat{w}(k) + L_w(y(k) - C\hat{x}(k)) \end{aligned} \tag{36}$$

where L_x and L_w are Luenberger observer gains of the state and disturbance respectively. Implementing the equations (36) to the augmented state-space mode (34), the output-feedback disturbance rejection controller based system is shown in the whole state-space form,

$$\begin{bmatrix} x(k+1) \\ w(k+1) \\ \hat{x}(k+1) \\ \hat{w}(k+1) \end{bmatrix} = \begin{bmatrix} \Phi & \Gamma & -\Gamma K & -\Gamma \\ 0 & 1 & 0 & 0 \\ L_xC & 0 & \Phi - L_xC - \Gamma K & 0 \\ L_wC & 0 & -L_wC & 1 \end{bmatrix} \begin{bmatrix} x(k) \\ w(k) \\ \hat{x}(k) \\ \hat{w}(k) \end{bmatrix} + \begin{bmatrix} \Gamma G \\ 0 \\ \Gamma G \\ 0 \end{bmatrix} r \tag{37}$$

Compared the equation (34) with the equation (27), the order of state space model increases from three to four, thus the number of poles of $\Phi - \Gamma K$ and $\Phi - LC$ of also need to be four. On the basis of the final choice of pole set 4, the poles of the state-feedback controller is as followed:

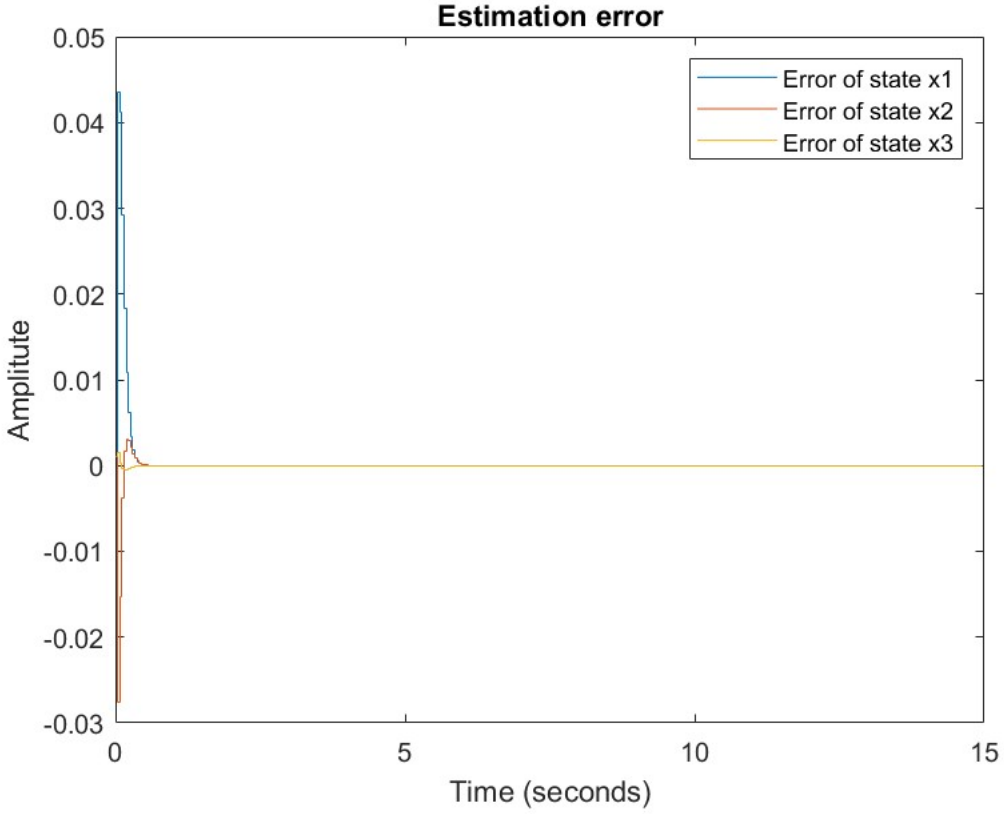

Fig. 22. Estimation error of states of the Output-Feedback servo tracking controller.

- Continuous time domain $poles_{statefeedback} = \begin{bmatrix}$-3.2155-3.3721i -3.2155 +3.3721i -10.0000$\end{bmatrix}$

According to the equation (24), the continuous time pole location of state-feedback controller $poles_{observer}$ can be transformed to the discrete-time pole location $poles_{observer}$

- Discrete-time domain $poles_{statefeedback} = \begin{bmatrix}$0.9984+0.0017i 0.9984-0.0017i 0.99$\end{bmatrix}$

Note that when discretizing the disturbance rejection controller, the sampling time h is different from that of the tracking controller. The corresponding state-feedback gain is $K = \begin{bmatrix} 0.7388 & -12.4952 & -195.1584 & * \end{bmatrix}$. The fourth element of state-feedback gain can be assigned freely because it cannot influence the eigenvalue decided by the disturbance dynamics $w(k+1) = w(k)$. By comparing different values of the fourth element of K, finally we choose $K = \begin{bmatrix} 0.7388 & -12.4952 & -195.1584 & 0.05 \end{bmatrix}$. The output-feedback gain is designed by placing the location of poles of $\Phi - LC$. The poles of observer is chosen as:

- Continuous time domain $poles_{observer} = \begin{bmatrix}$-21 -22 -23 -575.4$\end{bmatrix}$

According to the equation (24), the continuous time pole location of the observer $poles_{observer}$ can be transformed to the discrete-time pole location $poles_{observer}$ as

- Discrete-time domain $poles_{observer} = \begin{bmatrix} 0.9896 & 0.9891 & 0.9886 & 0.75 \end{bmatrix}$

It is worth mentioning that the fourth observer pole cannot be designed by state pole since the the disturbance $w(k)$ is not controllable and thus it is not affected in the feedback gain K. Thus considering the convergence rate of disturbance dynamics, we assign the fourth pole to the location 0.75 (discrete-time domain), which makes sure the disturbance dynamics converge more rapidly than both the dynamics of estimation error and dynamics of the response to input.

By choosing the initial state $x_0 = \begin{bmatrix} 0.001 & 0.001 & 0.001 & 1 \end{bmatrix}$ for the system and initial state $x_0 = \begin{bmatrix} 0 & 0 & 0 & 0 \end{bmatrix}$ for the observer, the step responses of system output, observer output are shown in figure

(23) respectively. The peak existing in the curve of step responses attributes to the disturbance of the system and the derivation of initial states of system output from observer output which lead to longer duration time. When time is larger than 0.8 sec, the system and observer system are almost identical, which shows the nice performance of observer. Thus taking into account the performance of estimation error of states, it can be concluded that the observer design is an ideal estimate of all the states: the observer can reduce the error of states by capturing the dynamics of the real states.

In figure (24), it compares the derivation of estimated states from the real states. The estimation error of states x_1, x_2 and x_3 converges to zero until achieving the time point $t = 1.08$.

(a) duration time $= 0.336$ sec

(b) Amplitude of the system output y caused by disturbance q: 0.5532

(c) steady output $y = 0$

which satisfies the control objectives of Output-Feedback disturbance rejection controller.

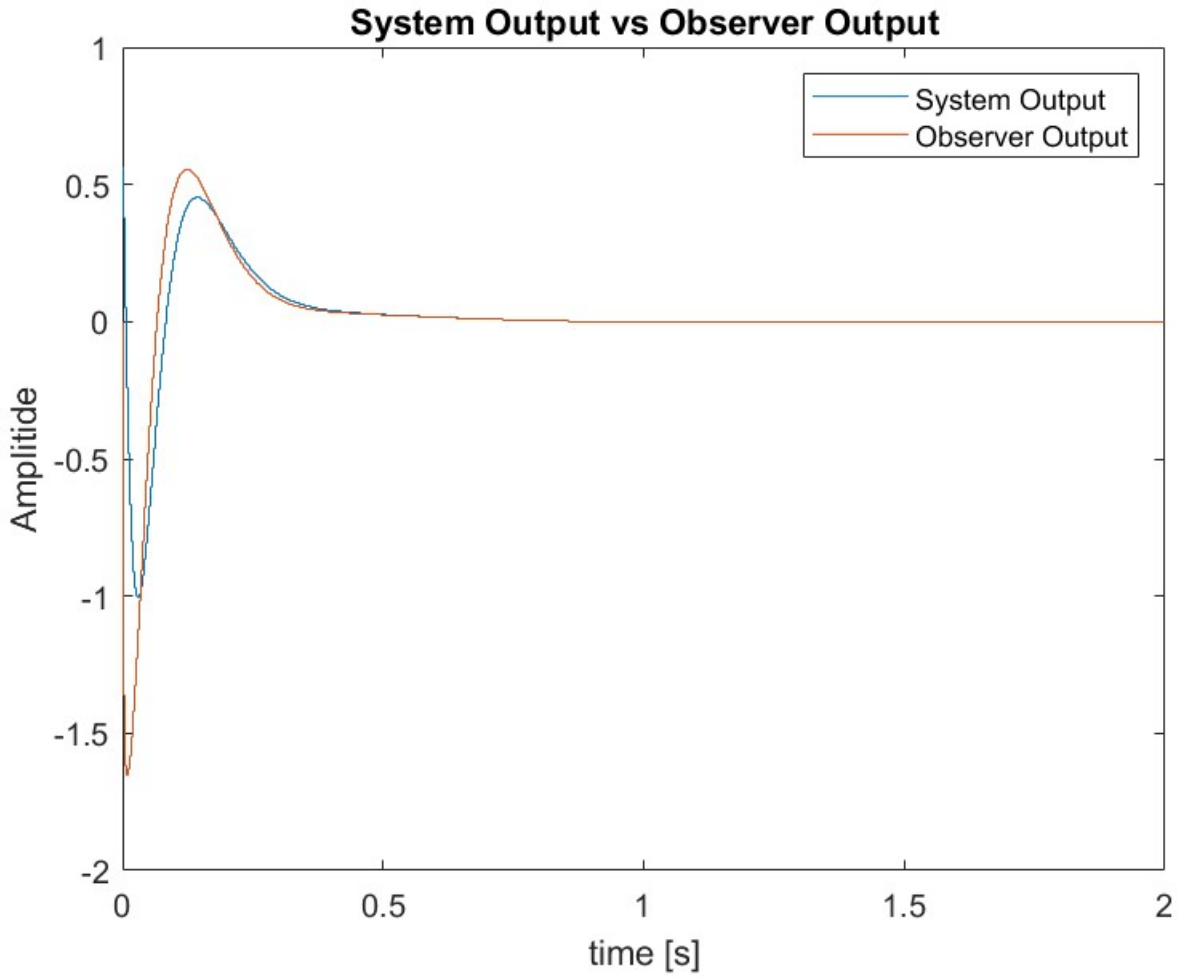

Fig. 23. Step responses of original system and observer system.

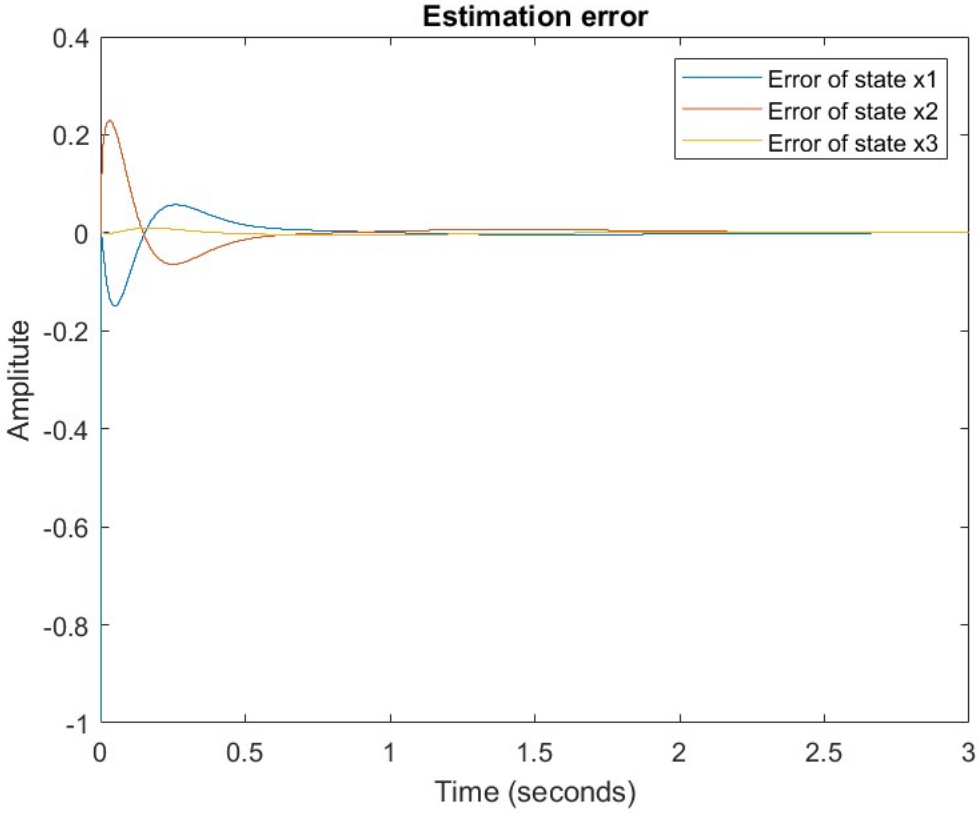

Fig. 24. Estimation error of states of the Output-Feedback disturbance rejection controller.

VI. LQ CONTROLLER

In this section, the discrete-time Linear Quadratic controller is designed to minimize the the cost J function which compensates the speed of the state response and the effort of control action. The cost function J is given in the equation (38)

$$J = \sum_{k=0}^{N-1} x^T(k)Q_1x(k) + 2x^T(k)Q_3u\,(k) + u^T(k)Q_2u(k) + x^T(N)Q_0x(N) \tag{38}$$

where Q_1, Q_3, Q_2, Q_0 are weighting matrices. Based on the assumptions of the solvability of LQ problem, Q_1 and Q_2 are positive semi-definite. For computational simplification, we assume Q_1 and Q_2 are diagonal matrices and Q_3 and Q_0 are zero. Q_1 is 3×3 which matches the degree of the state vector $x(k)$,

$$Q_1 = \begin{bmatrix} Q_{11} & 0 & 0 \\ 0 & Q_{22} & 0 \\ 0 & 0 & Q_{33} \end{bmatrix} \tag{39}$$

. Q_2 is one-dimensional scalar. Overall, there are four parameters Q_{11}, Q_{22}, Q_{33} and Q_2 which can influence the minimization of cost function J. In order to compare the influence of weighting elements Q_{11}, Q_{22} and Q_{33} in the matrix Q_1 and weighting matrix Q_2 on the cost function J, one of the four elements takes all the values in the set $\begin{bmatrix} 0.01 & 1 & 100 & 10000 \end{bmatrix}$ and the other three elements are all set to be 1. In Fig 26, it deduced that the influence of elements Q_{11}, Q_{22}, Q_{33} and Q_2 are quite different to the LQ reference tracking response. For Q_{11} element, by increasing the value of it from 0.01 to 10000,

although the overshoot decrease with the increase of the value, from 21.8% to 4.72%, it has to pay the price to the much larger rise time from 0.453 sec to 1.36 sec, which drags the speed of the LQ reference tracking response to the large extent. Also, for the value of $Q_{11} = 0.01$ and $Q_{11} = 0.1$, the LQ reference tracking responses are almost identical, it is worth mentioning that in order to minimize the cost function J the values of Q_{11}, Q_{22}, Q_{33} and Q_2 should be as small as possible, thus we choose $Q_1 = 0.01$.

Now taking a look at Q_{22} element, when increasing the value of Q_{22} to 10000, the shape of LQ reference tracking changes significantly with the overshoot decreasing to 0. The rise time of LQ reference tracking when $Q_{22} = 10000$ is only 0.83 sec, which is much smaller that the former experiment of which the rise time is 1.36 sec. Thus it is worth the price to choose $Q_{22} = 10000$ to obtain zero overshoot with the cost of having the rise time at 0.83 sec.

For the element Q_{33}, the shape of reference tracking changes slightly when the value reaching 10000, for the values 0.01, 1 and 100, the shape of LQ reference tracking responses do not change obviously. Therefore it is proper to choose $Q_{33} = 0.01$.

For Q_2 element, when increasing the value of Q_2 from 0.01 to 1, the rise time of LQ reference tracking decreases from 0.458 sec to 0.306, with the overshoot increasing from 12.4% to 21.8%, when keep on increasing the value of Q_2 element, the overshoot and rise time do not change a lot, which means the optimal value of Q_2 element is either 0.01 or 1. In order to choose Q_2 from 0.01 and 1, we did an experiment with fixed $Q_{11} = 0.01$, $Q_{22} = 10000$ and $Q_{33} = 0.01$, and comparing the values of Q_2 from 0.01 and 1, shown in figure (25). It is easily observed that when $Q_2 = 1$ the LQ reference tracking has quicker response compared with the case of $Q_2 = 0.01$ (having 2.93 sec of rise time), only having 0.418 sec of rise time.

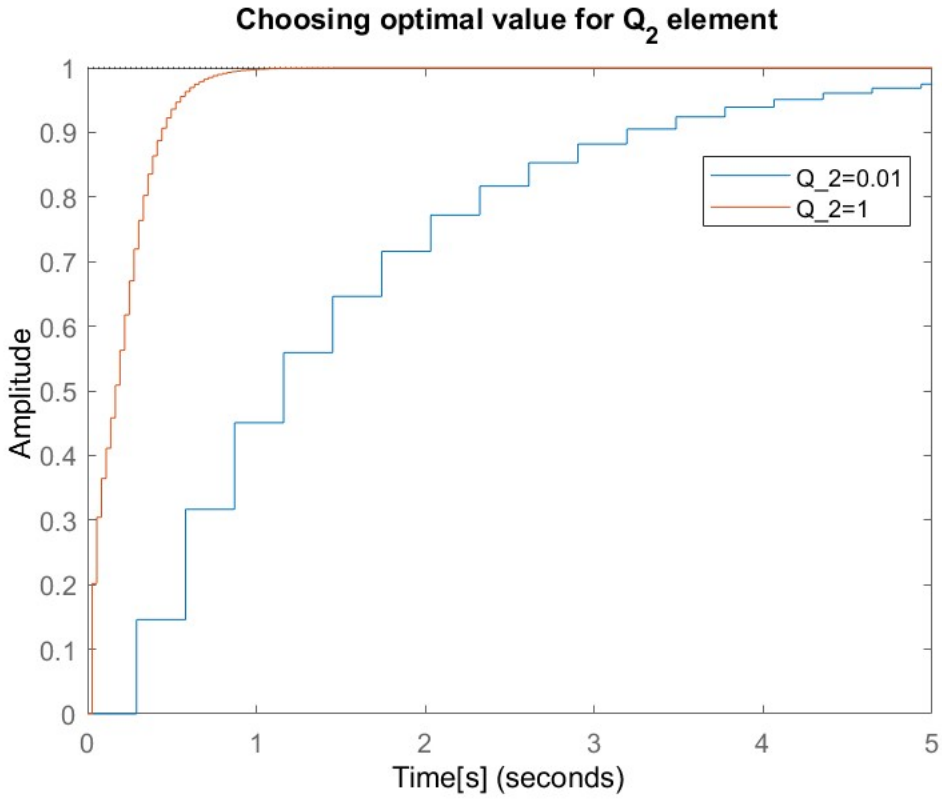

Fig. 25. Comparison of LQ reference tracking responses with different values of Q_2 element.

In order to achieve the high speed of step response and at the same time reduce the overshoot of the step response to satisfy the control objectives, the final choice of matrices Q_1 and Q_2 are,

$$Q_1 = \begin{bmatrix} 0.01 & 0 & 0 \\ 0 & 10000 & 0 \\ 0 & 0 & 0.01 \end{bmatrix} \qquad (40)$$
$$Q_2 = 1$$

The final LQ reference tracking response is shown in Fig 27, and the performance of LQ controller is
(a) settling-time $= 0.672$ sec
(b) rise-time $= 0.418$ sec
(c) overshoot $= 0\%$
(d) steady-state error $= 0$
which satisfies the control objectives of reference tracking controller.

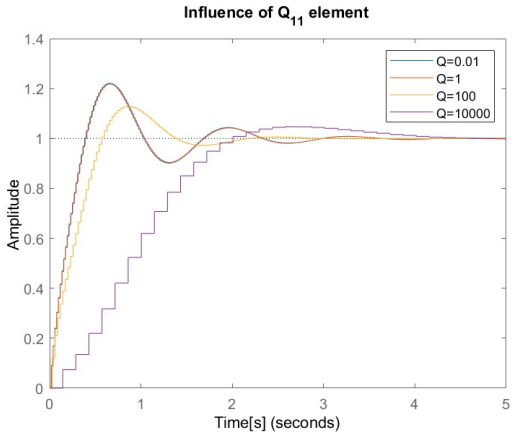

(a) Influence of Q_{11} element.

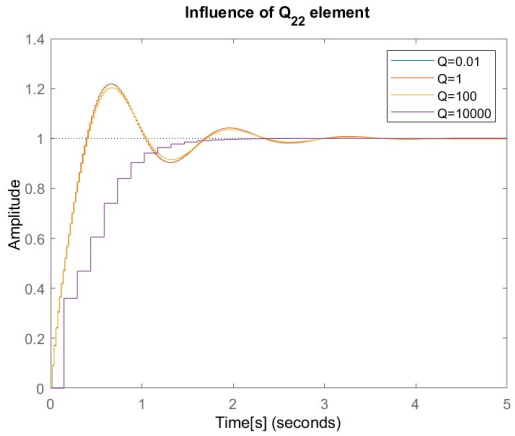

(b) Influence of Q_{22} element.

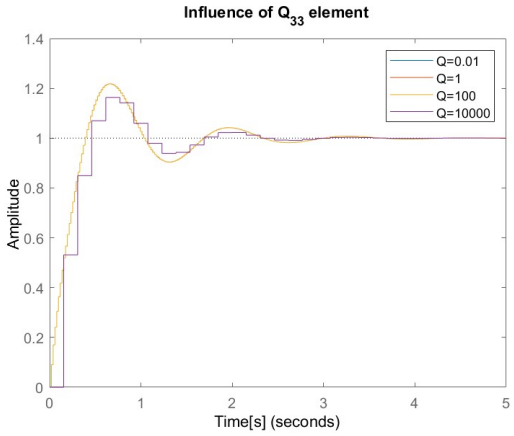

(c) Influence of Q_{33} element.

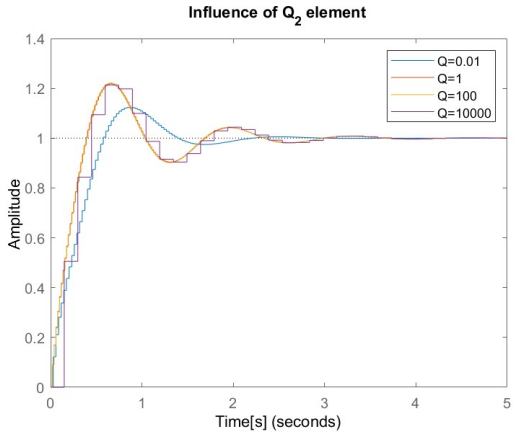

(d) Influence of Q_2 element.

Fig. 26. Compare the influence of different elements Q_{11}, Q_{22}, Q_{33} and Q_2 on the performance of LQ reference tracking response.

VII. Control Input Analysis

In this section, the focus is put on the boundaries of control input. In practical controller design, the input signal is usually under some limitations because the real actuator usually has certain physical

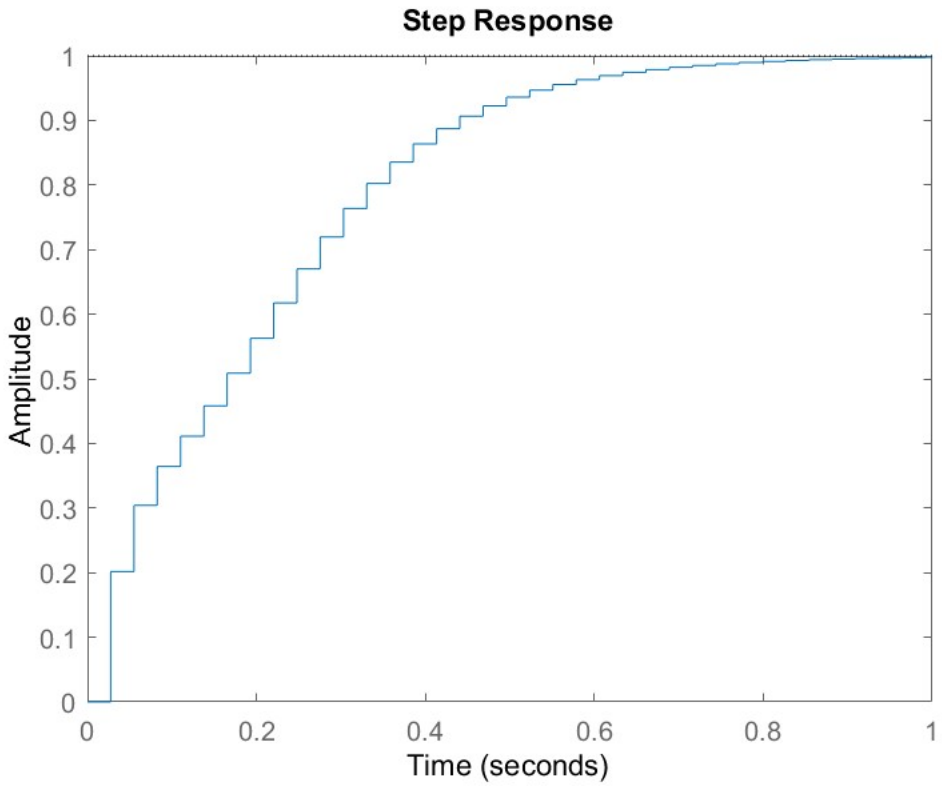

Fig. 27. Step response of the final LQ controller.

limitation. Starting from this part, the control input is set in the boundary of $[-2, 2]$ with the avoidance of actuator saturation.

A. *Control input of PID controller*

In order to obtain the control input, the model in simulink is built to get the control input of PID controller for reference tracking, shown in figure (28). In figure (29), it shows that the control input of PID controller for reference tracking stays in the range of $[-2, 2]$, with the highest value of 1 and lowest value around -0.4, which helps to avoid the actuator saturation.

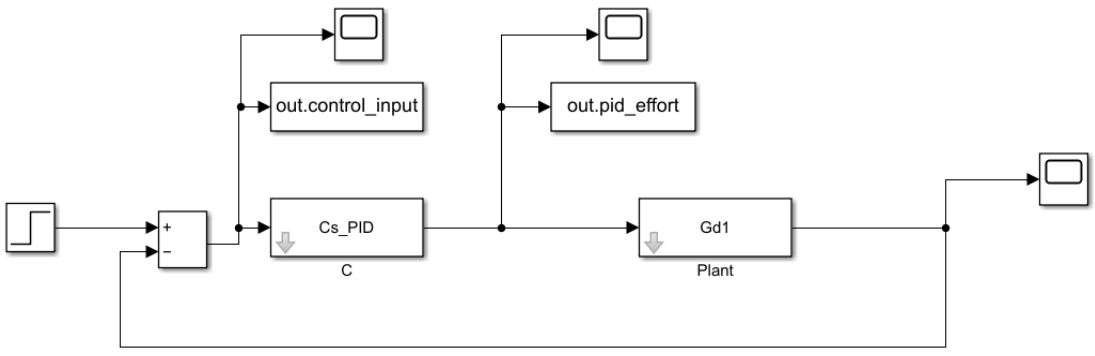

Fig. 28. The model consists of PID controller for reference tracking.

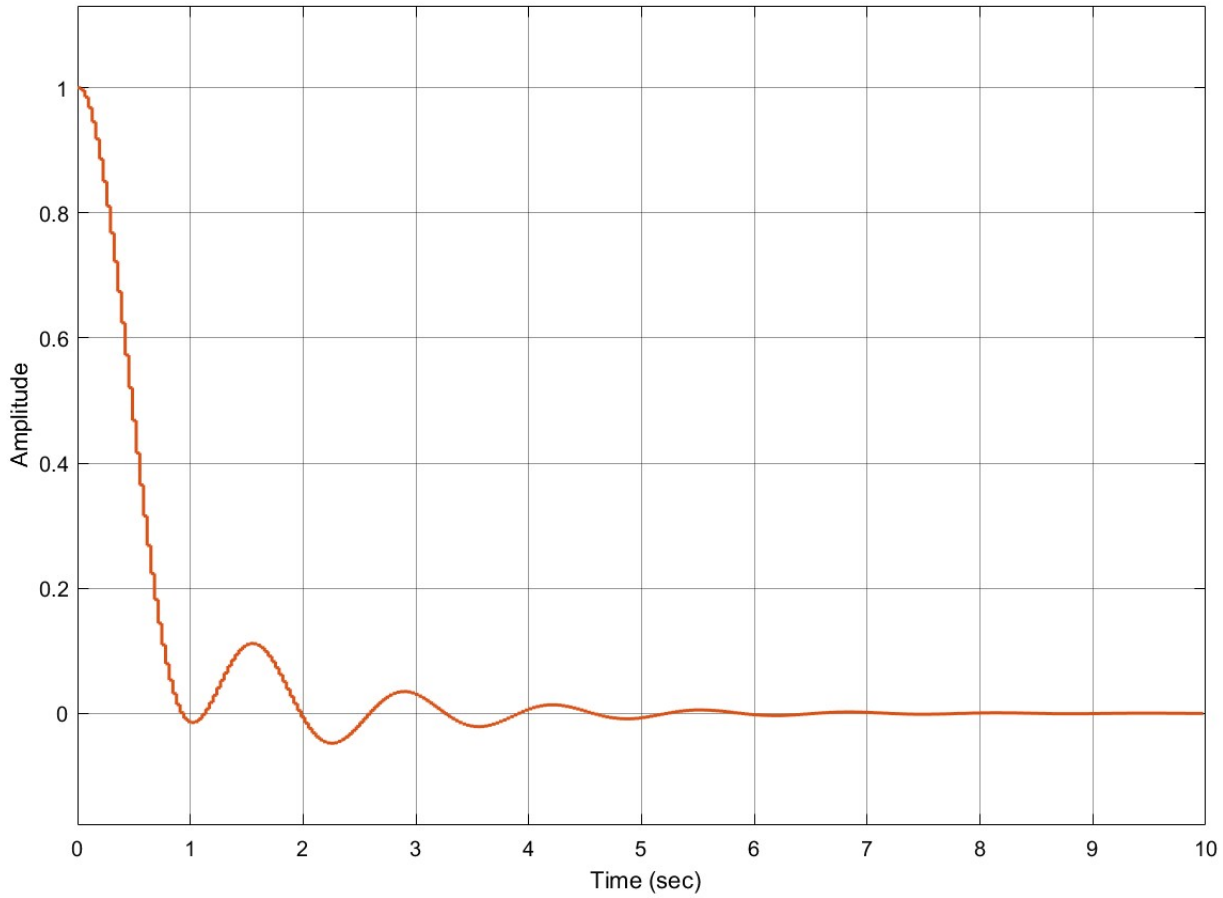

Fig. 29. Control input of PID controller for reference tracking.

For the model built for disturbance rejection is shown in figure (30). In figure (31), it shows that the control input of PID controller for disturbance rejection stays in the range of $[-2, 2]$, with the highest value of 0 and lowest value around $-8.6 \cdot 10^{-3}$, which helps to avoid exceeding the limit of input boundaries.

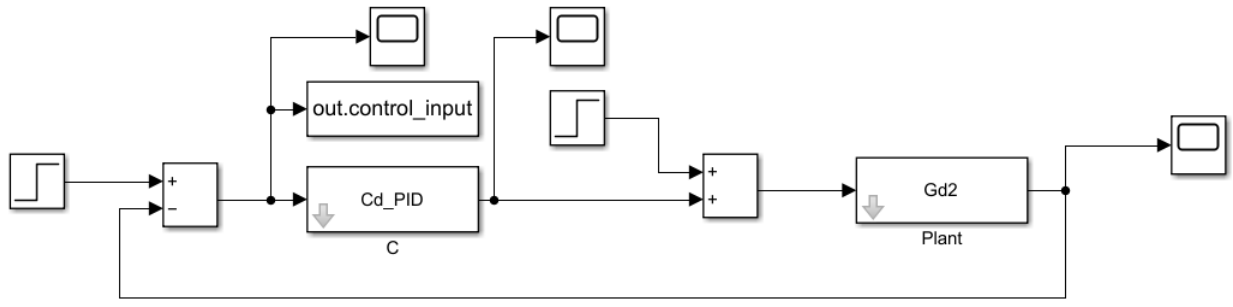

Fig. 30. Control input of PID controller for disturbance rejection.

B. Control input of State-Feedback controller

In figure (32), it illustrates the input signal of state-feedback controller does stay inside the set of $[-2, 2]$.

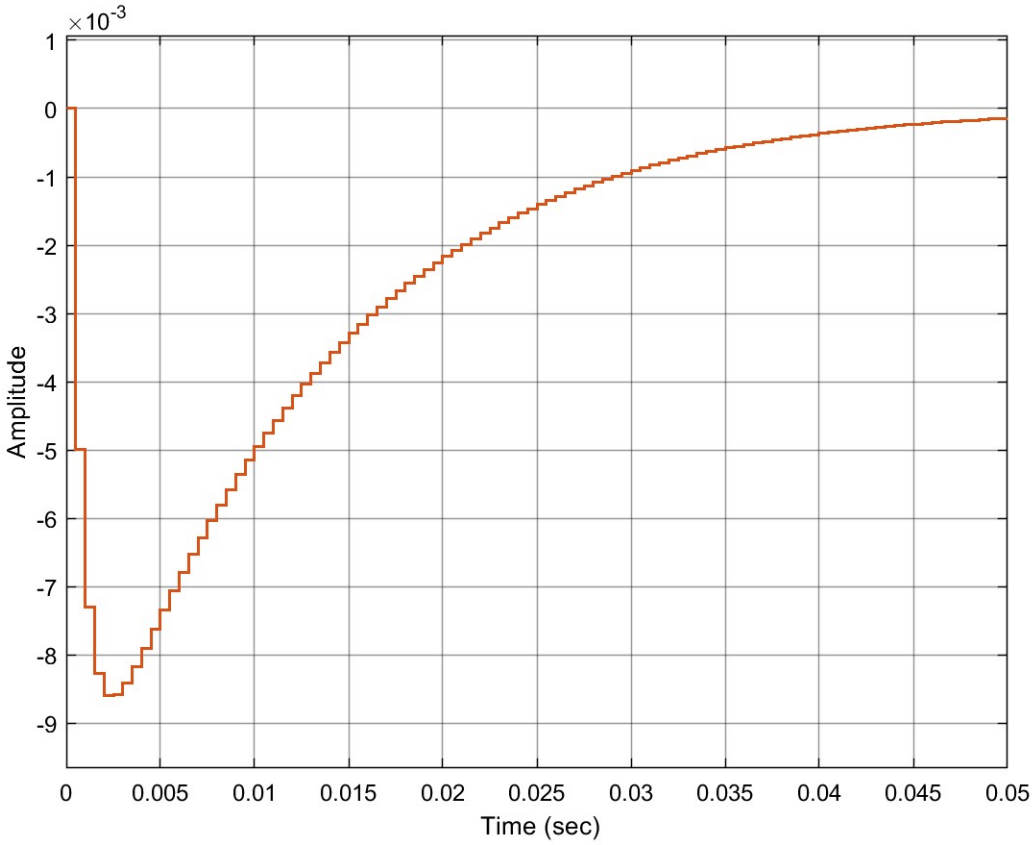

Fig. 31. Control input of PID controller for disturbance rejection.

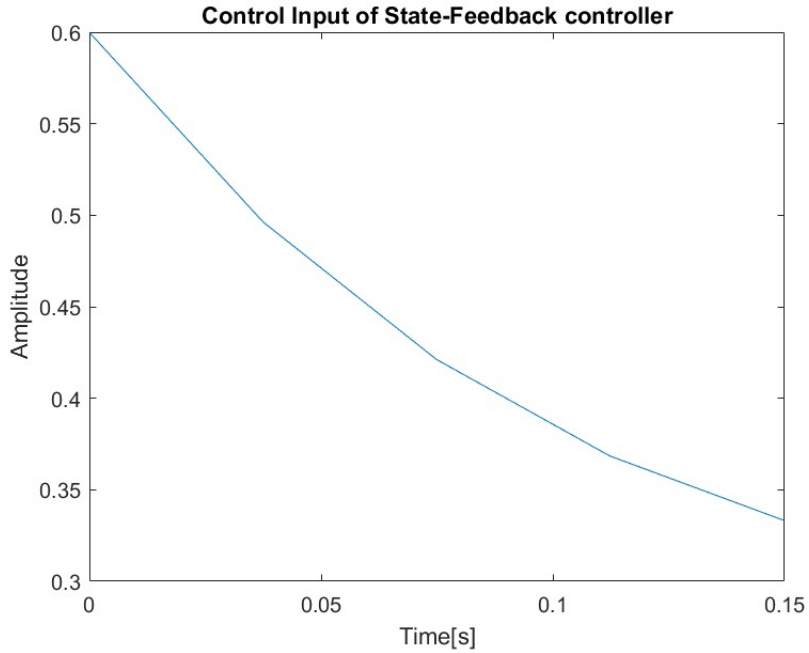

Fig. 32. Control input of state-feedback controller.

C. Control input of Output-Feedback controller

The input signal of Output-Feedback controller for reference tracking stays in the input boundaries $[-2, 2]$, with the largest value of 0.51 and the smallest value of 0.37. The input signal of Output-Feedback controller for disturbance rejection exceeds input boundaries $[-2, 2]$, with the largest value of 16.22 and the smallest value of -13.93.

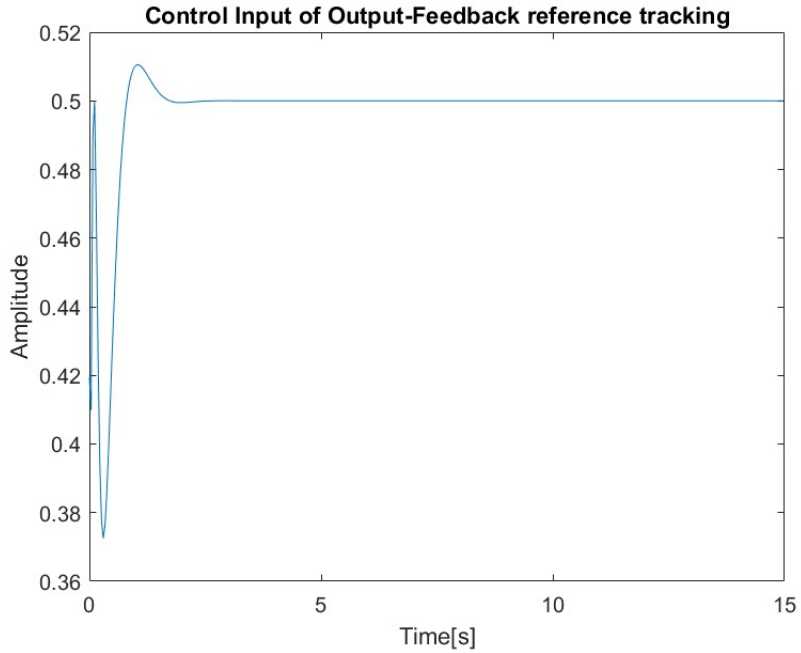

Fig. 33. Control input of output-feedback controller for reference tracking.

D. Control input of LQ controller

The input signal of LQ controller stays in the input boundaries $[-2, 2]$, with the largest value 0.5 and the smallest value 0.23.

VIII. Redesign Controller

In practical control design, the input of actuator has the input limitation to avoid saturation. In this assignment the input boundaries are set to $[-2, 2]$.

A. Redesign of discrete-time control

As shown in figures (29) and (31), the inputs of PID controllers all sit in the boundaries of $[-2, 2]$. Thus the focus should be placed on the enhancement of performance of the PID controllers, i.e. smaller overshoot and less settling time.

1) Redesign of discrete-time reference tracking controller: The redesigned reference tracking controller is designed as:

$$C(s) = 0.85\frac{s + 14}{s(s + 13.5)} \tag{41}$$

Note that the integer part $\frac{1}{s}$ is fixed, the only trick we tune the PID controller for reference tracking is the lag compensator. By moving the zero and pole of lag compensator along the left direction of real axis, the step response shows a good performance of less overshoot and settling time.

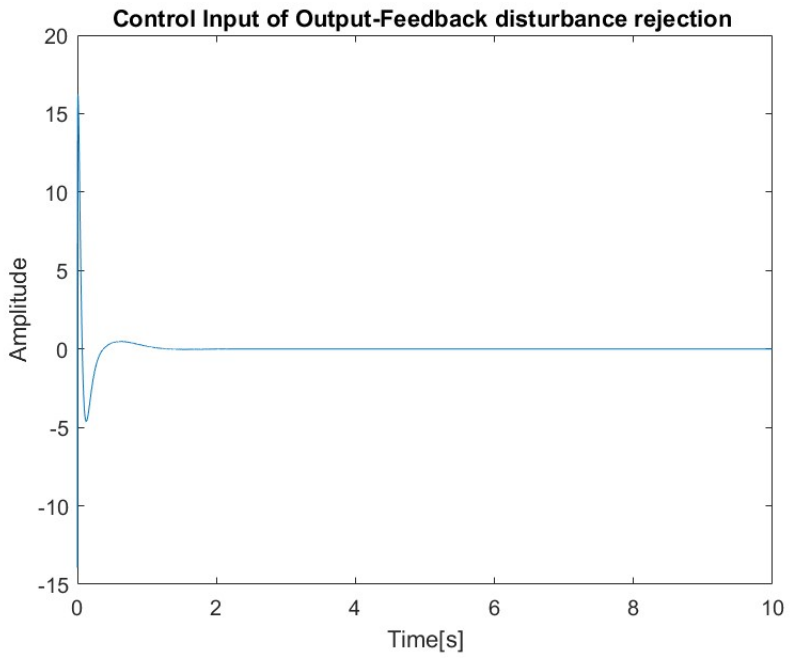

Fig. 34. Control input of output-feedback controller for disturbance rejection.

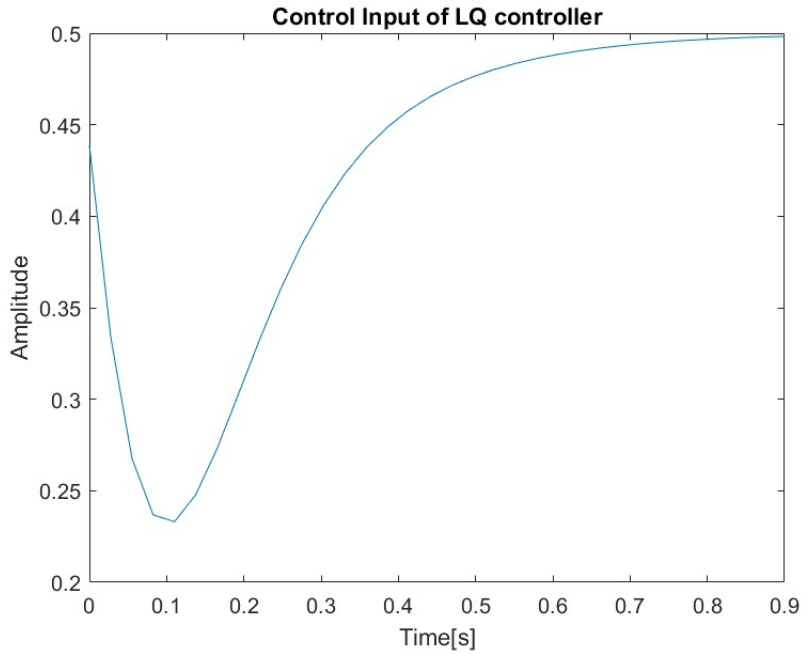

Fig. 35. Control input of LQ controller.

The step response of redesign PID reference tracking controller compared with the previous PID reference tracking controller is shown in figure (36). It can observed that the redesigned PID reference tracking controller has faster step response and smaller overshoot.

The control performance of the redesigned reference tracking PID controller is shown as:

(a) settling-time $= 3.06$ sec

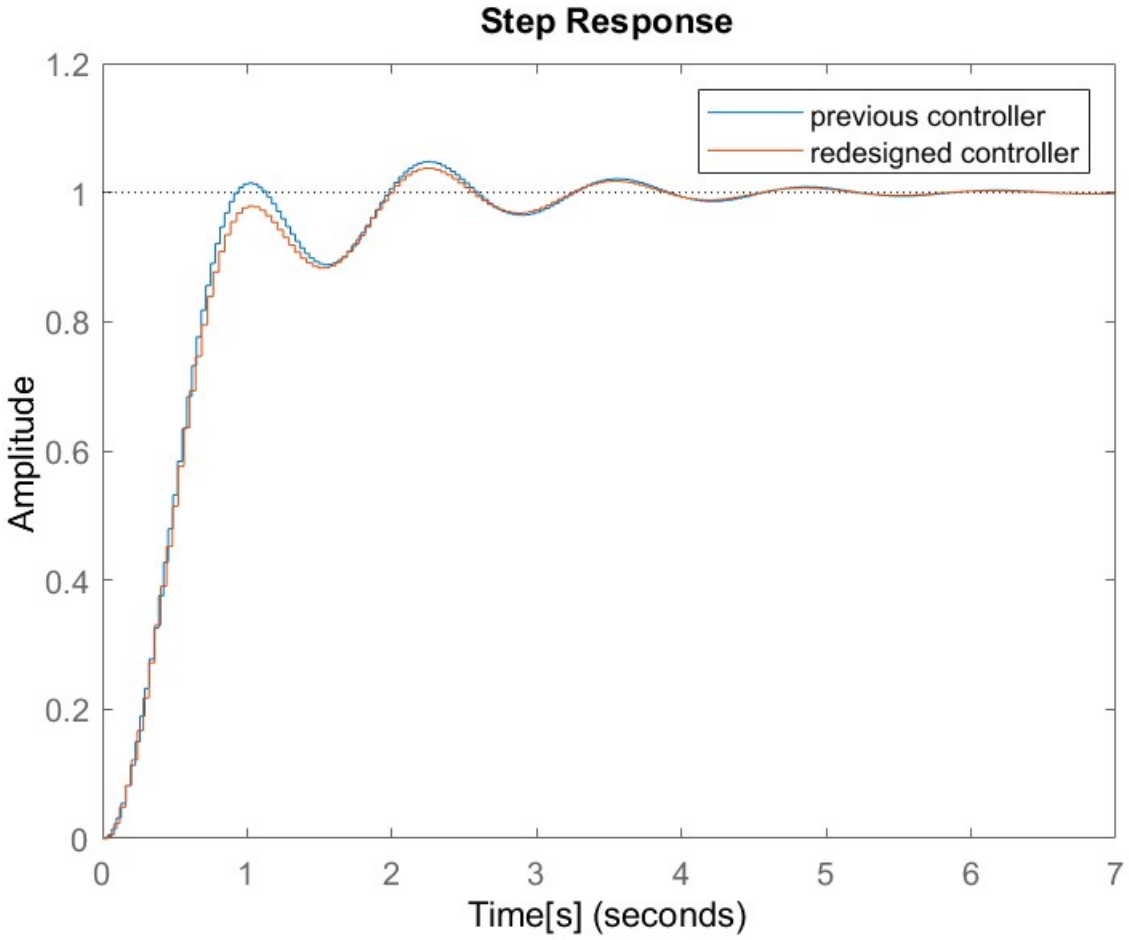

Fig. 36. Redesign PID reference tracking controller compared with the previous PID reference tracking controller.

(b) overshoot $= 3.75\%$
(c) steady-state error $= 0$

which satisfies the control objectives of reference tracking controller. At the same time, the redesigned reference tracking PID controller has better performance than the previous PID controller with overshoot decreasing from 4.78% to 3.75% and settling time decreasing from 3.61 to 3.06 sec.

2) Redesign of discrete-time reference tracking controller: In order to decrease the overshoot of the step response and speed up the response, the strategies could be increase the K_P, K_D and K_I parameters of PID controller.

The redesigned PID disturbance rejection controller is designed as:

$$C(s) = 150 + \frac{12000}{s} + \frac{20}{100s + 1} \tag{42}$$

The step response of redesign PID disturbance rejection controller compared with the previous PID disturbance rejection is shown in figure (37). It can observed that the redesigned PID disturbance rejection controller has faster step response and smaller overshoot.

The control performance of the redesigned disturbance rejection PID controller is shown as:

(a) duration time $= 0.0451$ sec

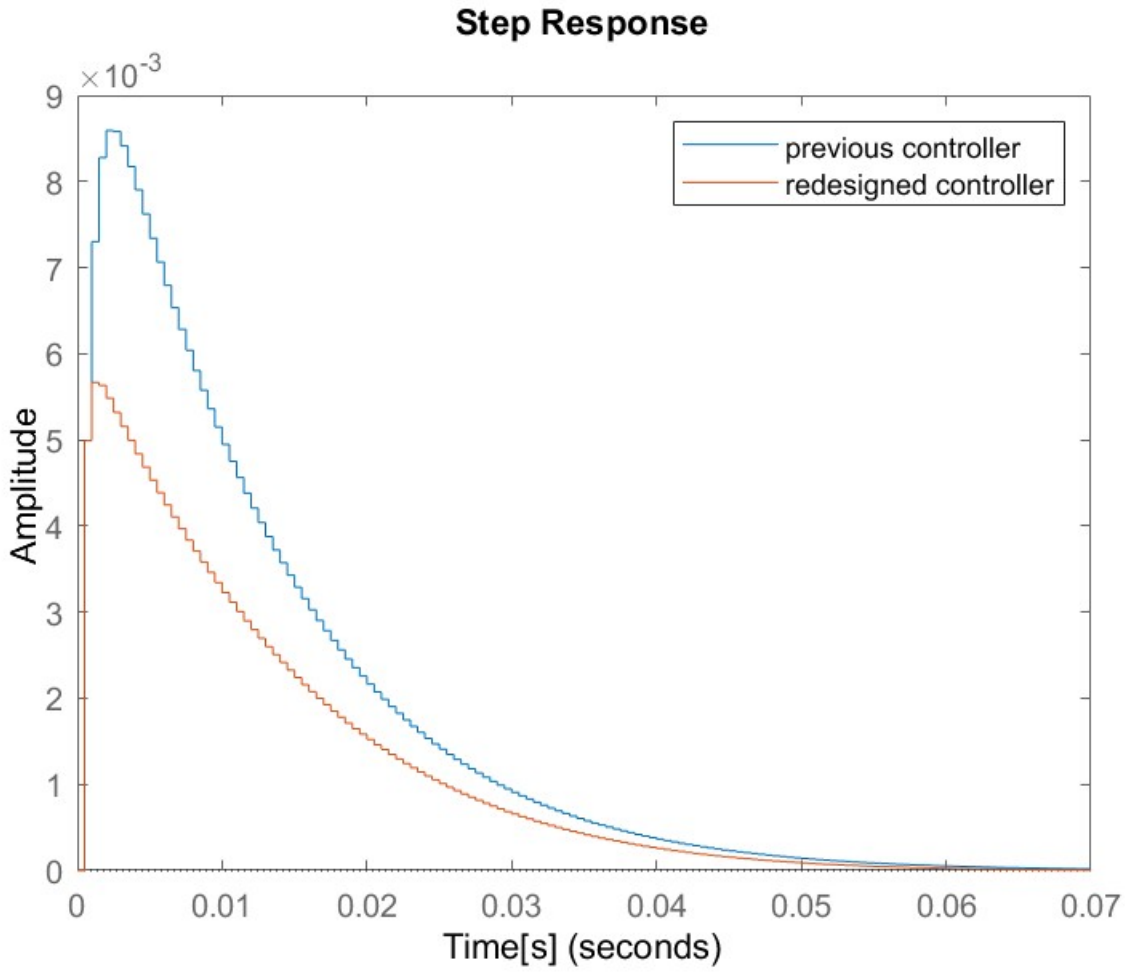

Fig. 37. Redesign PID disturbance rejection controller compared with the previous PID disturbance rejection controller.

(b) Amplitude of the system output y caused by disturbance q: 0.0015
(c) steady output $y = 0$

which satisfies the control objectives of Output-Feedback disturbance rejection controller. At the same time, the redesigned disturbance rejection PID controller has better performance than the previous PID controller with maximum amplitude decreasing from 0.00859 to 0.00567.

B. Redesign of Discrete-Time State-Feedback Pole Placement Control

In the pole placement design it is quite easy to reduce the control effort by slowing down the system response. The discrete-time pole placement is redesigned as $[0.8795 - 0.1116i, 0.8795 + 0.1116, 0.8]$. The step response of redesign discrete-time State-Feedback pole placement control compared with the previous discrete-time State-Feedback pole placement control is shown in figure (38). It can observed that the discrete-time State-Feedback pole placement control has faster step response and smaller overshoot.

The redesigned performance of State-Feedback pole placement control is

(a) settling-time $= 0.962$ sec
(c) overshoot $= 1.32\%$
(d) steady-state error $= 0$

which satisfies the control objectives of reference tracking controller with overshoot decreasing from 2.01% to 1.32% and settling time decreasing from 1.17 to 0.962 sec.

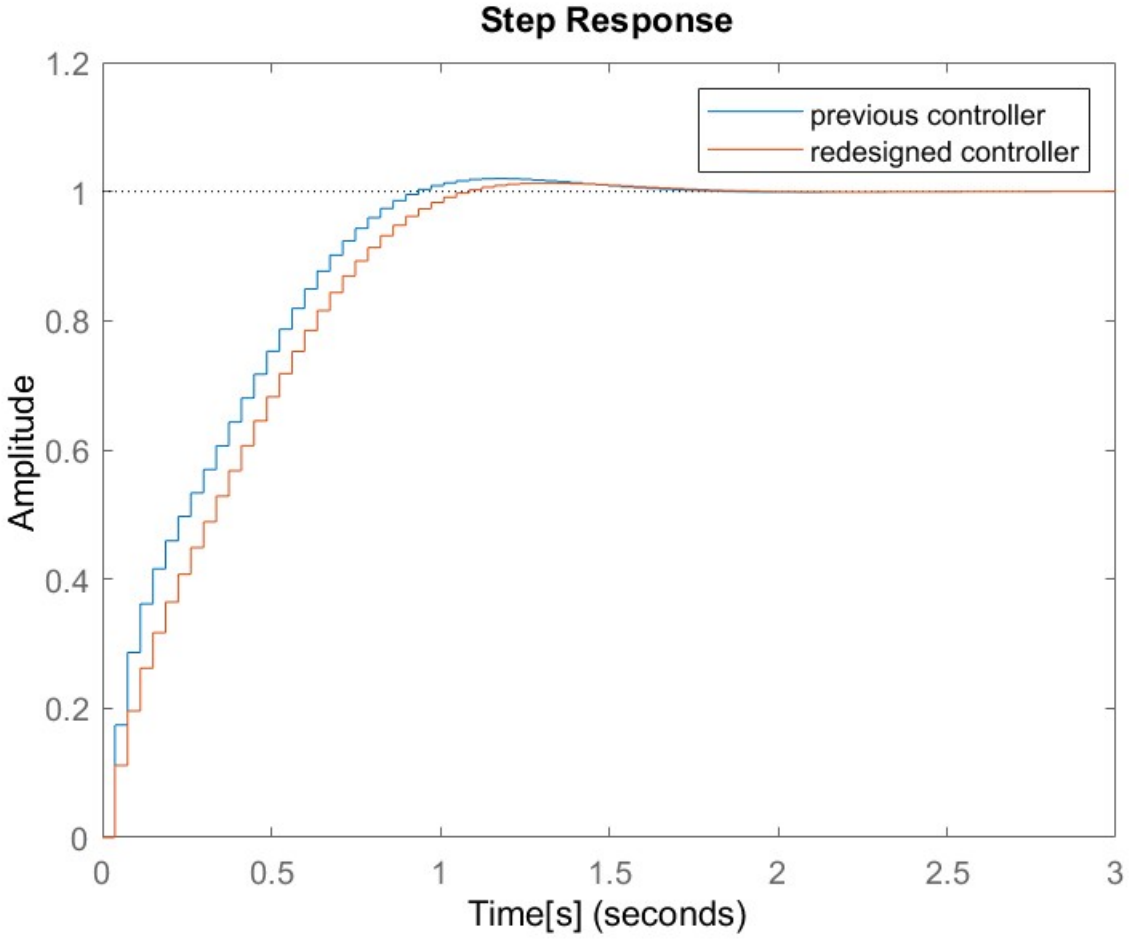

Fig. 38. Redesign of State-Feedback pole placement control compared with the previous State-Feedback pole placement control.

C. *Redesign of Discrete-Time LQ Control*

As shown in figure (35), the input of LQ control is in the boundaries of $[-2, 2]$. Therefore the focus should be placed on the enhancement of performance of the LQ controller, i.e. less settling time. According to former analysis, $Q_2 2$ element accounts for the largest loop shaping of step response, thus by changing the $Q_2 2$, the proper value for $Q_2 2$ can be found as 6500, in order to achieve the high speed of step response to enhance the control performance.

The redesigned LQ controller has the matrices Q_1 and Q_2 as,

$$\begin{aligned} Q_1 &= \begin{bmatrix} 0.01 & 0 & 0 \\ 0 & 6500 & 0 \\ 0 & 0 & 0.01 \end{bmatrix} \\ Q_2 &= 1 \end{aligned} \tag{43}$$

The step response of redesigned LQ controller compared with previous LQ controller is shown in Fig 39, it is easily found that the redesigned LQ controller has faster speed of response compared with the previous LQ controller. More specifically, the redesigned performance of LQ controller is

(a) settling-time $= 0.484$ sec
(b) rise-time $= 0.342$ sec
(c) overshoot $= 0\%$
(d) steady-state error $= 0$

which satisfies the control objectives of reference tracking controller.

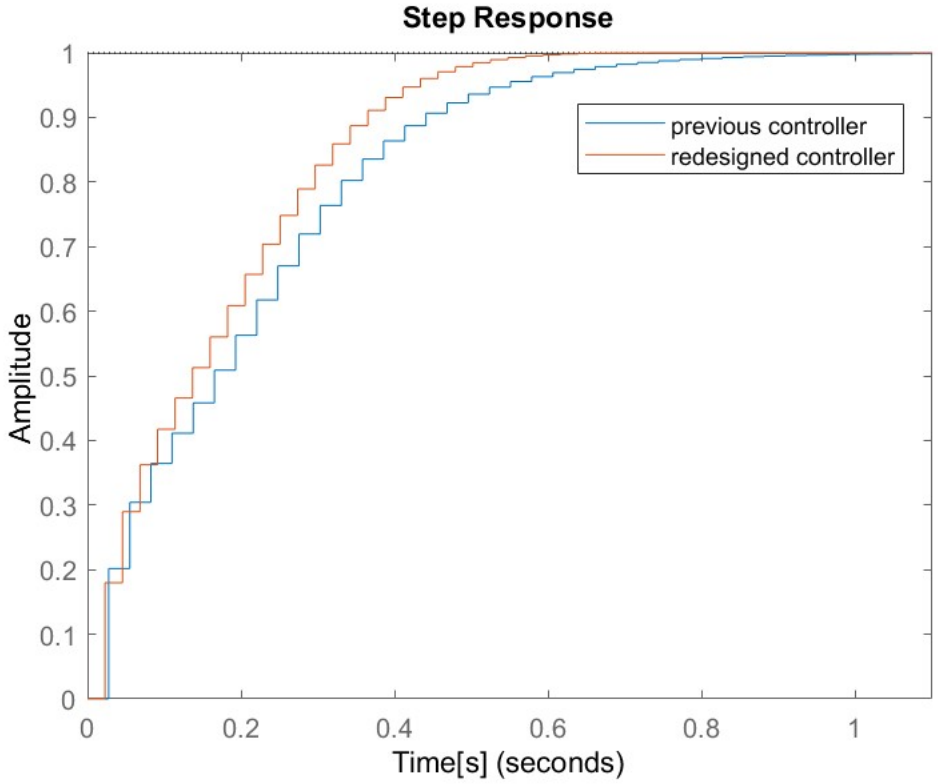

Fig. 39. : Redesign LQ controller compared with the previous LQ controller.

IX. Steady State Error Elimination

In this section, the analysis of elimination of steady state error is implemented. In section I, when designing the PID controller, the system is type 0 and thus it cannot track the step input without steady error. Based on this, the integrator of PID controller structure is necessary as it collects all the past values and has the function of a memory register. After adding the zero pole to the transfer function, the system becomes type 1, and this augmented system can thus reach the reference without any steady state error. When using the State-Feedback methods or Output-Feedback methods, commonly there exist steady-state error which stems the system to achieve the optimal input. Therefore the feed-forward gain G which is multiplied by the reference input in the structure (29) needs to be designed to eliminate the steady-state error. In MATLAB, this gain can be calculated as the inverse of dcgain of the whole system with the step input. The steady-state error can be compensated by the way of multiplying feed-forward gain with the

reference input Gr. The proof of the design of the feed-forward gain is shown as follows: Starting from the state-space model,

$$\begin{aligned} x(k+1) &= \Phi x(k) + \Gamma u(k) \\ y(k) &= Cx(k) \\ u(k) &= -Kx(k) + Gr \\ z(k) &= \tilde{C}x(k) + \tilde{D}u(k) \end{aligned} \tag{44}$$

The goal is that $z(k)$ tracks the $y(k)$ without any steady error input, in the form of $\lim_{k\to\infty} z(k) - r(k) = 0$. The $z(k)$ can be represented as,

$$z(k) = \tilde{C}x(k) + \tilde{D}(-Kx(k) + Gr) = (\tilde{C} - \tilde{D}K)x(k) + \tilde{D}Gr \tag{45}$$

In the scenario that the state $x(k)$ reach the steady state, the value of the state does not change anymore $x(k+1) = x(k)$, then the $x(k)$ can be written as

$$\begin{aligned} x(k) &= \Phi x(k) + \Gamma(-Kx(k) + Gr) \\ &= (I - (\Phi - \Gamma K))^{-1}\Gamma Gr \end{aligned} \tag{46}$$

Substituting (46) to (45), the $z(k)$ can be written as

$$z(k) = (\tilde{C} - \tilde{D}K)(I - (\Phi - \Gamma K))^{-1}\Gamma Gr + \tilde{D}Gr = ((\tilde{C} - \tilde{D}K)(I - (\Phi - \Gamma K))^{-1}\Gamma G + \tilde{D}G)r \tag{47}$$

Then the output is written as $y(k) = Cx(k) = C(I - (\Phi - \Gamma K))^{-1}\Gamma Gr$. As it is required to obtain the $\lim_{k\to\infty} z(k) - r(k) = 0$,

$$\lim_{k\to\infty} z(k) - r(k) = ((\tilde{C} - \tilde{D}K)(I - (\Phi - \Gamma K))^{-1}\Gamma G + \tilde{D}G)r - r = 0 \tag{48}$$

which infers $(\tilde{C} - \tilde{D}K)(I - (\Phi - \Gamma K))^{-1}\Gamma G + \tilde{D}G = I$. Taking the $\tilde{D} = 0$, the feed-forward gain can be written as $G = (C(I - (\Phi - \Gamma K))^{-1}\Gamma)^{-1}$. In MATLAB, this value can be calculated by applying the dcgain of the system

X. Time Delay Analysis

Time-delay often happens in real systems and will cause the phase shifts which will put constraint on the control bandwidth and affect closed-loop stability [1]. In this assignment, we only consider one-step delay situation. Starting from the state space model, the one-step delayed state space model is shown as

$$\begin{aligned} x(k+1) &= \Phi x(k) + \Gamma u(k-1) \\ y(k) &= Cx(k) \end{aligned} \tag{49}$$

Adding the dynamics of one-step time delayed input to (49), the state vector $x(k)$ extended to $\begin{bmatrix} x(k) & u(k-1) \end{bmatrix}^T$, the corresponding augmented state space model is obtained as

$$\begin{bmatrix} x(k+1) \\ u(k) \end{bmatrix} = \begin{bmatrix} \Phi & \Gamma \\ 0 & 0 \end{bmatrix} \begin{bmatrix} x(k) \\ u(k-1) \end{bmatrix} + \begin{bmatrix} 0 \\ 1 \end{bmatrix} u(k) \tag{50}$$

Compared with original matrix Φ, the extended matrix has the structure $\begin{bmatrix} \Phi & \Gamma \\ 0 & 0 \end{bmatrix}$, which adds the system one more eigenvalue $\lambda = 0$ to the matrix, and it is equivalent to add one more pole to the transfer function, which can be viewed as adding an integrator to the controller. In the z domain, the integrator has the form of z^{-1} also the z transform of input and output are shown as:

$$\begin{aligned} X(z) &= (zI - \Phi)^{-1}\Gamma z^{-1}U(z) \\ Y(z) &= CX(z) = C(zI - \Phi)^{-1}\Gamma z^{-1}U(z) \end{aligned} \tag{51}$$

A. Time delay for PID controller

According the former analysis, by adding the integrator to the controller, the controller has the property of time delay. In order to clarify this structure of time delay, we compare the original system and time delay system of reference tracking in simulink, shown in figure (40). The step responses of original system

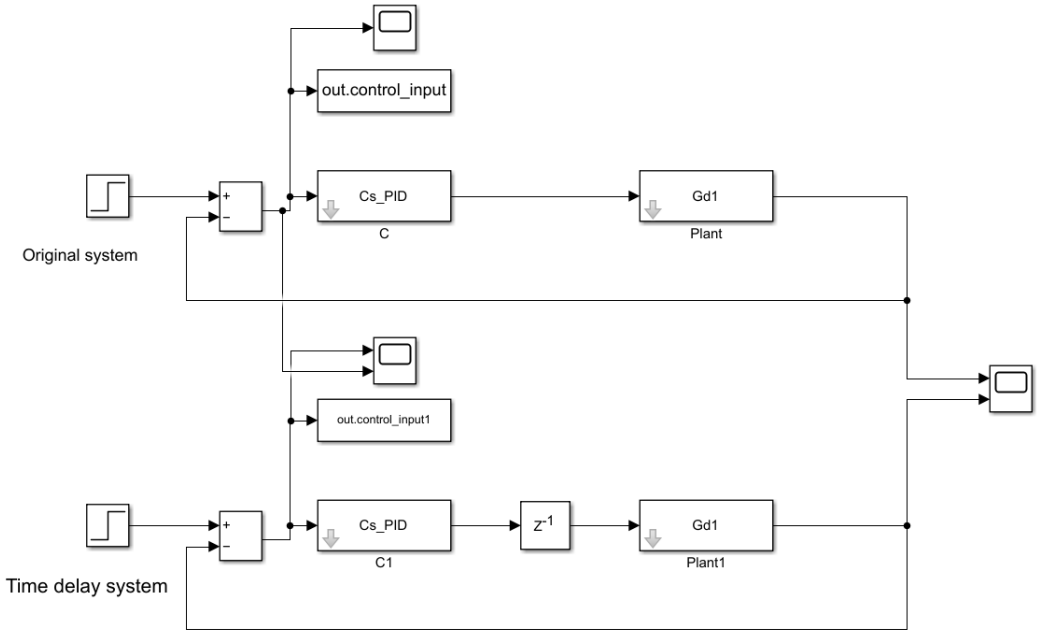

Fig. 40. Comparison of original system and time delay system of reference tracking.

and time delay system of reference tracking are shown in figure (41) It easily observed that after adding the time delay to the control input, the the delayed system is not just shifting the whole shape by one time step, but changing the shape itself as well. More specifically, the time shifted system has higher amplitude compared than the original system, probably due to changing the poles' location after adding the time delay part to the control input.

For the disturbance rejection system, similarly by adding the one time delay to control input, the model in simulink is shown in figure (42). The step responses of original system and time delay system of disturbance rejection are shown in figure (43). By adding the time delay part to the control input, the time delayed system has higher amplitude in comparision with the original system, with the highest amplitude of around $12 \cdot 10^{-3}$ to $8 \cdot 10^{-3}$, which is induced by the variation of pole location.

B. Time delay for State-Feedback controller

By adding the time delay dynamics to the system, the augmented state vector is written as $f(k) = \begin{bmatrix} x(k) & u(k-1) \end{bmatrix}$, the state feedback controller is designed as

$$u(k) = -K_f f(k) + Gr \tag{52}$$

The new state space model is represented as

$$\begin{bmatrix} x(k+1) \\ u(k) \end{bmatrix} = \begin{bmatrix} \Phi & \Gamma \\ -K_x & -K_u \end{bmatrix} \begin{bmatrix} x(k) \\ u(k-1) \end{bmatrix} + \begin{bmatrix} 0 \\ G \end{bmatrix} r \tag{53}$$

where K_x and K_u are the decomposition of K_f, K_x is three dimensional vector, consisting of the first three elements of K_f, K_u is the scalar having the value of the fourth element of K_f.

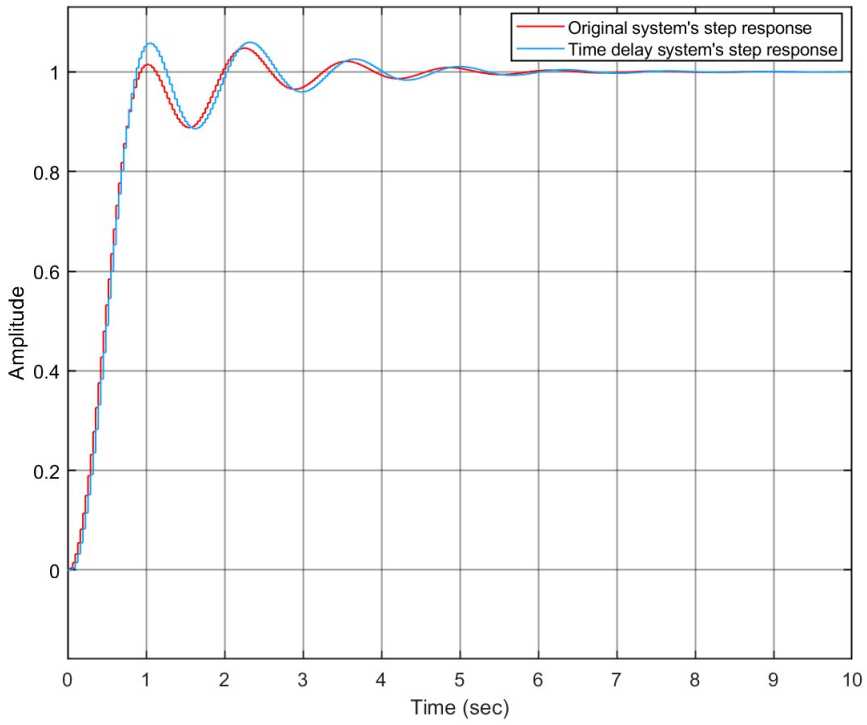

Fig. 41. Step responses of original system and time delay system of reference tracking.

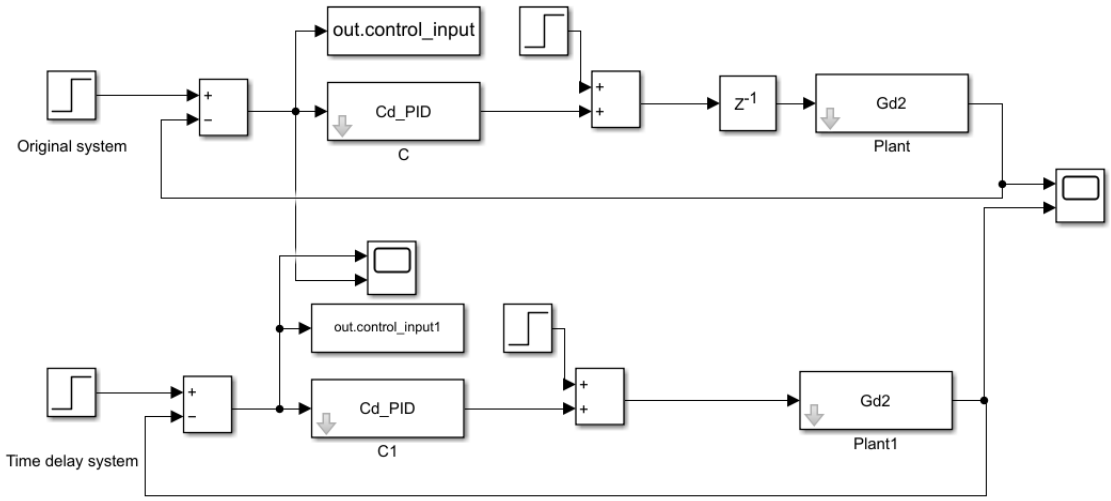

Fig. 42. Step responses of original system and time delay system of disturbance rejection.

The discrete-time poles location was chosen to be $pd = [0.6624, 0.6381, 0.6147, 0.5]$. The step responses of time delayed State-Feedback control system and original system are shown in figure (44). It can be observed that the time delayed system responds slower than the original system. At the same time, the shape of the time delayed step response changes due to the variation of location of poles.

C. Time delay for Output-Feedback controller

1) Time delay for Output-Feedback controller for reference tracking: By adding the input delay to the whole system $u(k) = -K_f f(k) + Gr$, the dynamics of Output-Feedback reference tracking system is

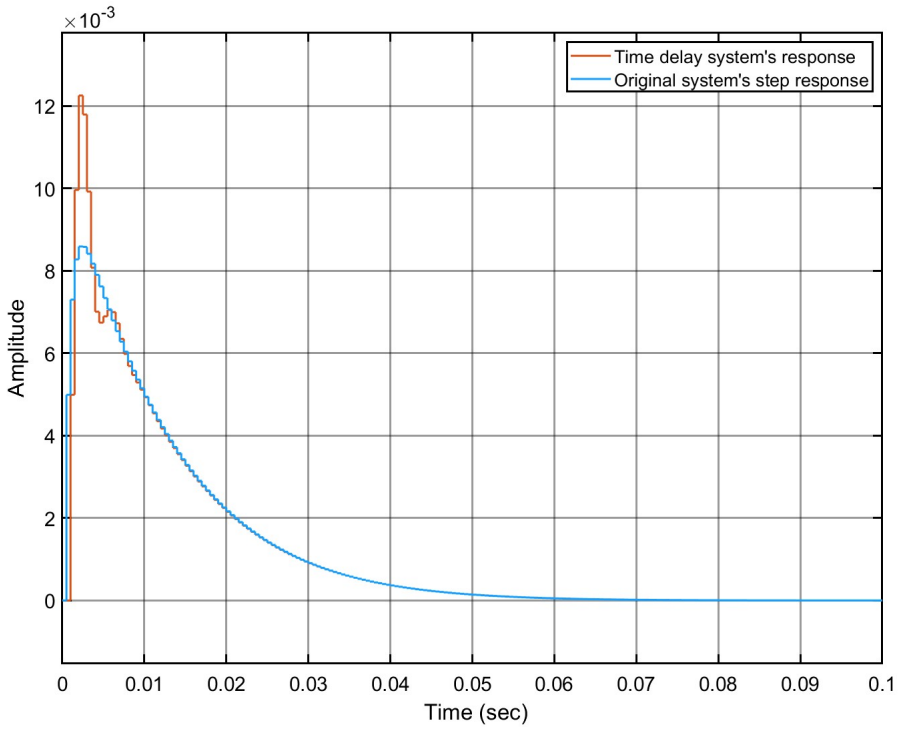

Fig. 43. Step responses of original system and time delay system of disturbance rejection.

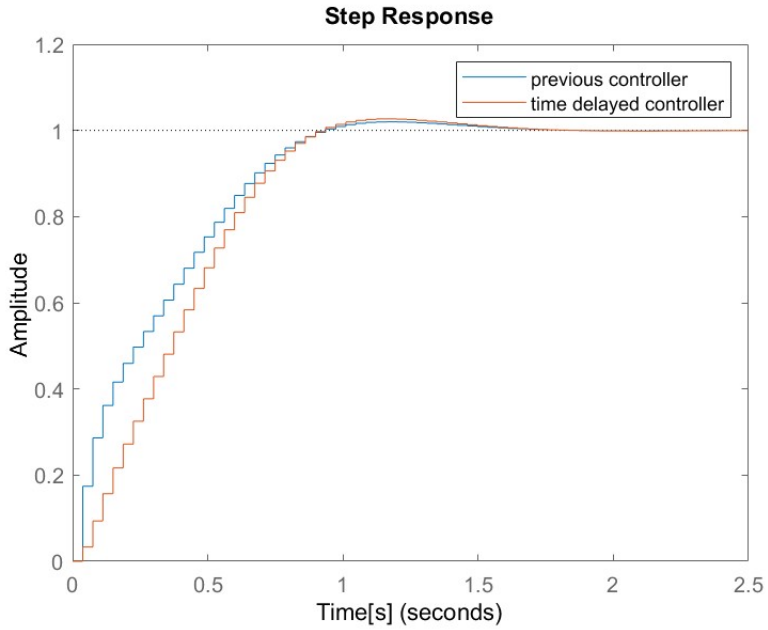

Fig. 44. .Step responses of time delayed State-Feedback control system and original system

written as

$$\begin{bmatrix} x(k+1) \\ u(k) \\ \hat{x}(k+1) \end{bmatrix} = \begin{bmatrix} \Phi & 0_{3\times 1} & -\Gamma K \\ 0_{1\times 3} & -K_u & -K_x \\ LC & 0_{3\times 1} & \Phi - \Gamma K - LC \end{bmatrix} \begin{bmatrix} x(k) \\ u(k-1) \\ \hat{x}(k) \end{bmatrix} + \begin{bmatrix} \Gamma G \\ G \\ \Gamma G \end{bmatrix} r \tag{54}$$

The step responses of time delayed Output-Feedback control system for reference traccking and original system are shown in figure (45). It can be observed that the time delayed system responds slower than the original system. At the same time, the shape of the time delayed step response changes due to the variation of location of poles.

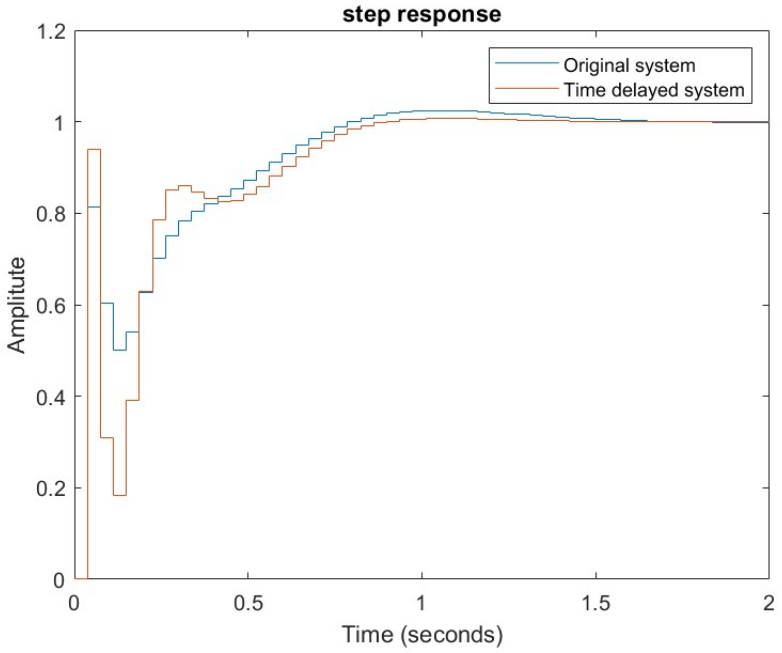

Fig. 45. .Step responses of time delayed Output-Feedback control system for reference tracking and original system

2) Time delay for Output-Feedback controller for disturbance rejection: By adding the input delay to the whole system $u(k) = -K_f f(k) - \hat{w}(k) + Gr$, the dynamics of Output-Feedback disturbance rejection system is written as

$$\begin{bmatrix} x(k+1) \\ w(k+1) \\ \hat{x}(k+1) \\ \hat{w}(k+1) \\ u(k) \end{bmatrix} = \begin{bmatrix} \Phi & \Gamma & -\Gamma K & -\Gamma & 0 \\ 0_{1\times 3} & 1 & 0_{1\times 3} & 0 & 0_{3\times 1} \\ L_x C & 0_{3\times 1} & \Phi - L_x C - \Gamma K & 0_{3\times 1} & 0_{3\times 1} \\ L_w C & 0 & -L_w C & 1 & 0 \\ 0_{1\times 3} & 0 & -K_x & -1 & -K_u \end{bmatrix} \begin{bmatrix} x(k) \\ w(k) \\ \hat{x}(k) \\ \hat{w}(k) \\ u(k-1) \end{bmatrix} + \begin{bmatrix} \Gamma G \\ 0 \\ \Gamma G \\ 0 \\ G \end{bmatrix} r \tag{55}$$

The step responses of time delayed Output-Feedback control system for disturbance rejection and original system are shown in figure (46). It can be observed that the time delayed system responds slower than the original system. At the same time, the shape of the time delayed step response changes due to the variation of location of poles.

D. Time delay for LQ controller

After implementing the input dynamics, the state vector augmenting from $x(k)$ to $f(k)$ the weighting matrix Q_1 has extended to Q_f with dimension 4. The Q_2 matrix is still scalar but has the new form of matrix Q_u.

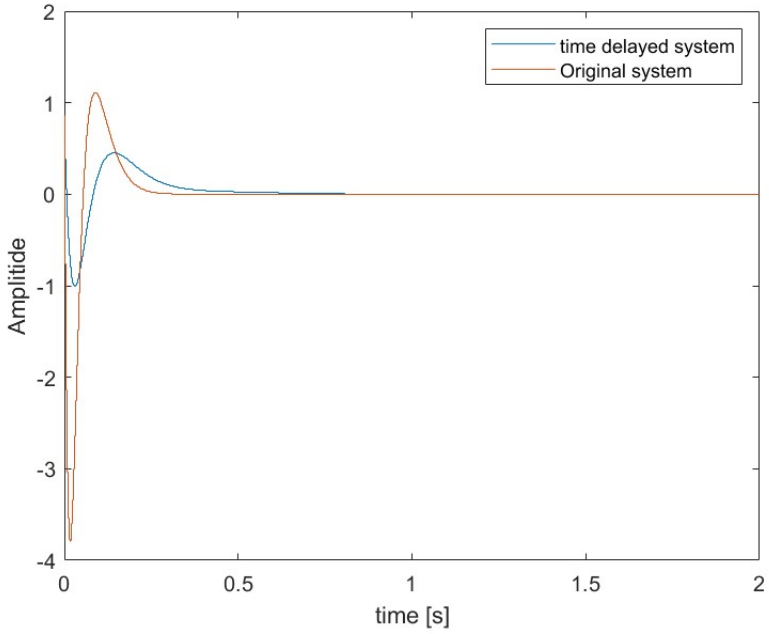

Fig. 46. .Step responses of time delayed Output-Feedback control system for disturbance rejection and original system

The new weighting matrices Q_f and Q_u have the form of:

$$Q_f = \begin{bmatrix} 0.01 & 0 & 0 & 0 \\ 0 & 6500 & 0 & 0 \\ 0 & 0 & 0.01 & 0 \\ 0 & 0 & 0 & 1 \end{bmatrix} \tag{56}$$
$$Q_u = 1$$

The step responses of time delayed LQ control system for disturbance rejection and original system are shown in figure (47). It can be observed that the time delayed system responds slower than the original system. At the same time, the shape of the time delayed step response changes due to the variation of location of poles.

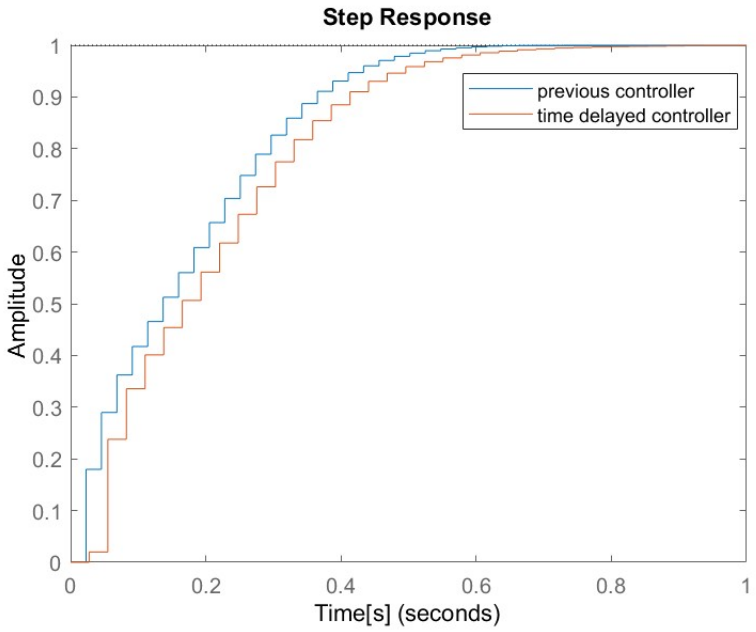

Fig. 47. .Step responses of time delayed LQ control system and original system

XI. CONCLUSION

This assignment provides us with the servo control system which is analyzed by different types of controllers including PID type controllers, State-Feedback controllers, Output-Feedback controllers and LQ controllers.

The first section consists of the design of PID type controller, which combines the analysis of both time domain and frequency domain to achieve the control objectives. It is divided into two parts to consider two different systems: reference tracking system and disturbance rejection system.

The second section puts focus on the discretization of the system. It analyzed two formulas of choice the sampling time and applied the strategies to the two systems mentioned before.

The third section was designed to construct the state output control system by using the pole placement method. It compared the performance four poles sets and chose the optimal one as the final state feedback controller.

The fourth section was about the design of Output Feedback controller. It designed the structures of the Output Feedback control based on reference tracking and disturbance rejection respectively. For disturbance rejection model, the disturbance dynamics is added to the system, which augmented the system's state space model.

The fifth section built the control system based on LQ control. The cost function was constructed to balance the speed of state response and the effort of control action. By building up the weighting matrices and analyzing the effect of each element of the weighting matrices to the step response, the optimal LQ weighting matrices were chosen as the final choice.

Control input analysis, redesign of all the controllers mentioned above, steady state error elimination and time delay analysis were shown in sections 6, 7, 8 and 9 respectively.

These sections took into account the physical limitations, i.e. the actuator' input boundaries in avoidance of saturation and common issue of time delay cases.

Overall, all the types of controllers were designed to meet the control requirements and were enhanced

according to the physical limitations.

REFERENCES

[1] Analyzing Control Systems with Delays - MathWorks. Retrieved from https://nl.mathworks.com/help/control/ug/analyzing-control-systems-with-delays.html